4. Phenomenology of proton-proton collisions

4.1 Introduction

4.2 Hard scattering formalism

4.3 Parton distribution functions

4.4 Soft proton-proton interactions

4.1 Introduction

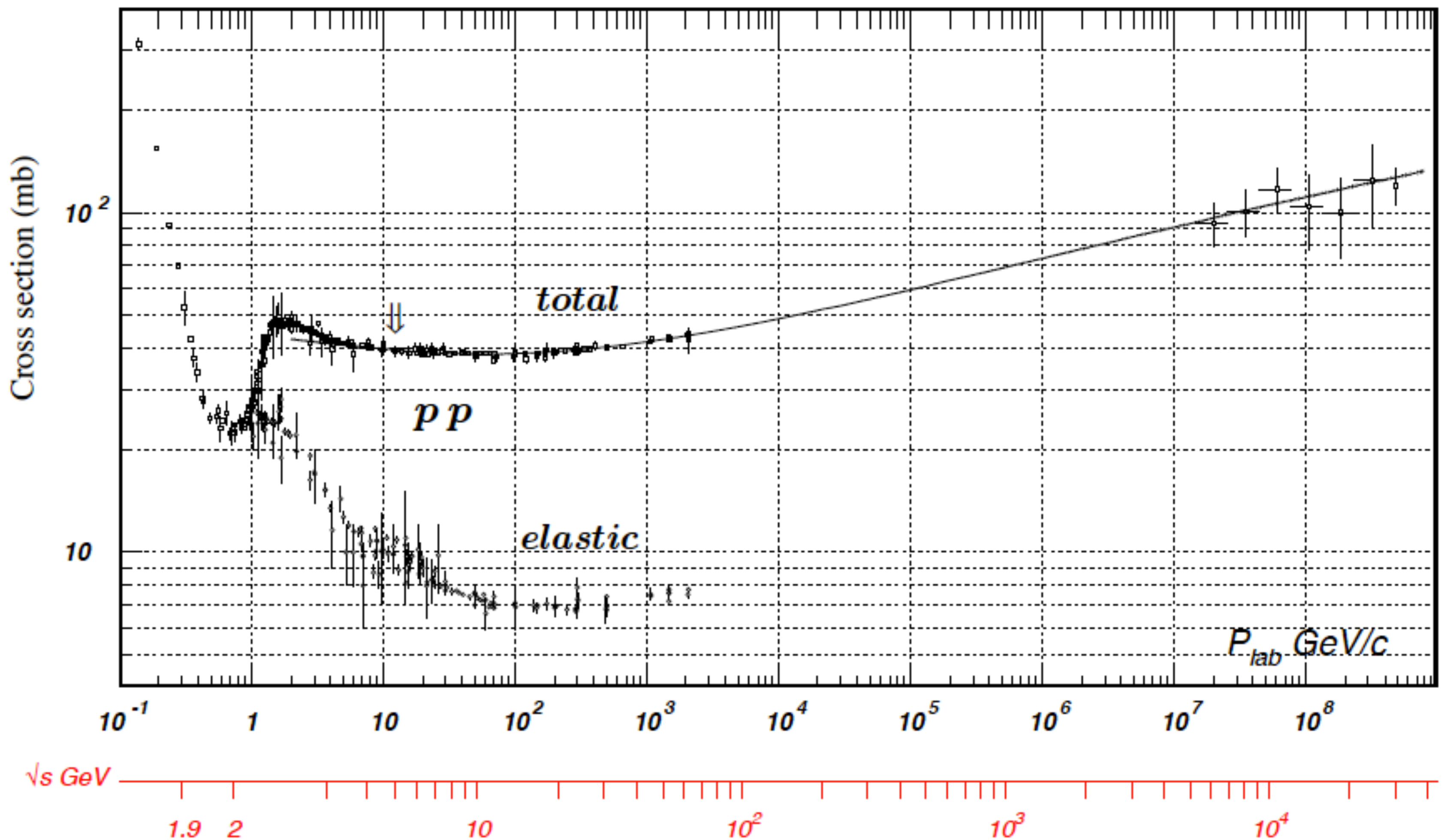

Total and elastic cross section for pp collisions as a function of the laboratory beam momentum and and the total centre-of-mass energy (Particle data group).

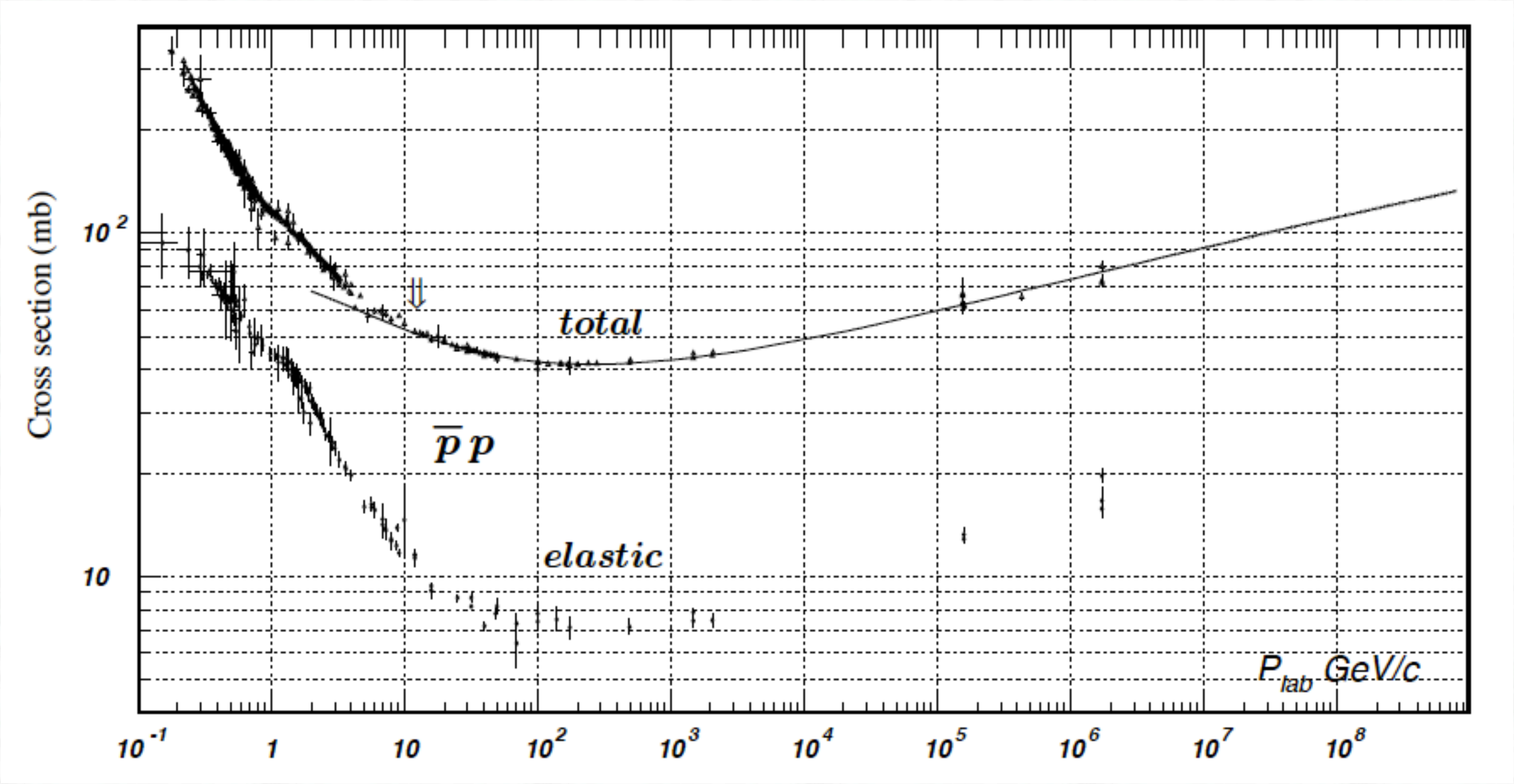

Total and elastic cross section for proton-antiproton collisions as a function of the laboratory beam momentum and and the total centre-of-mass energy (Particle data group).

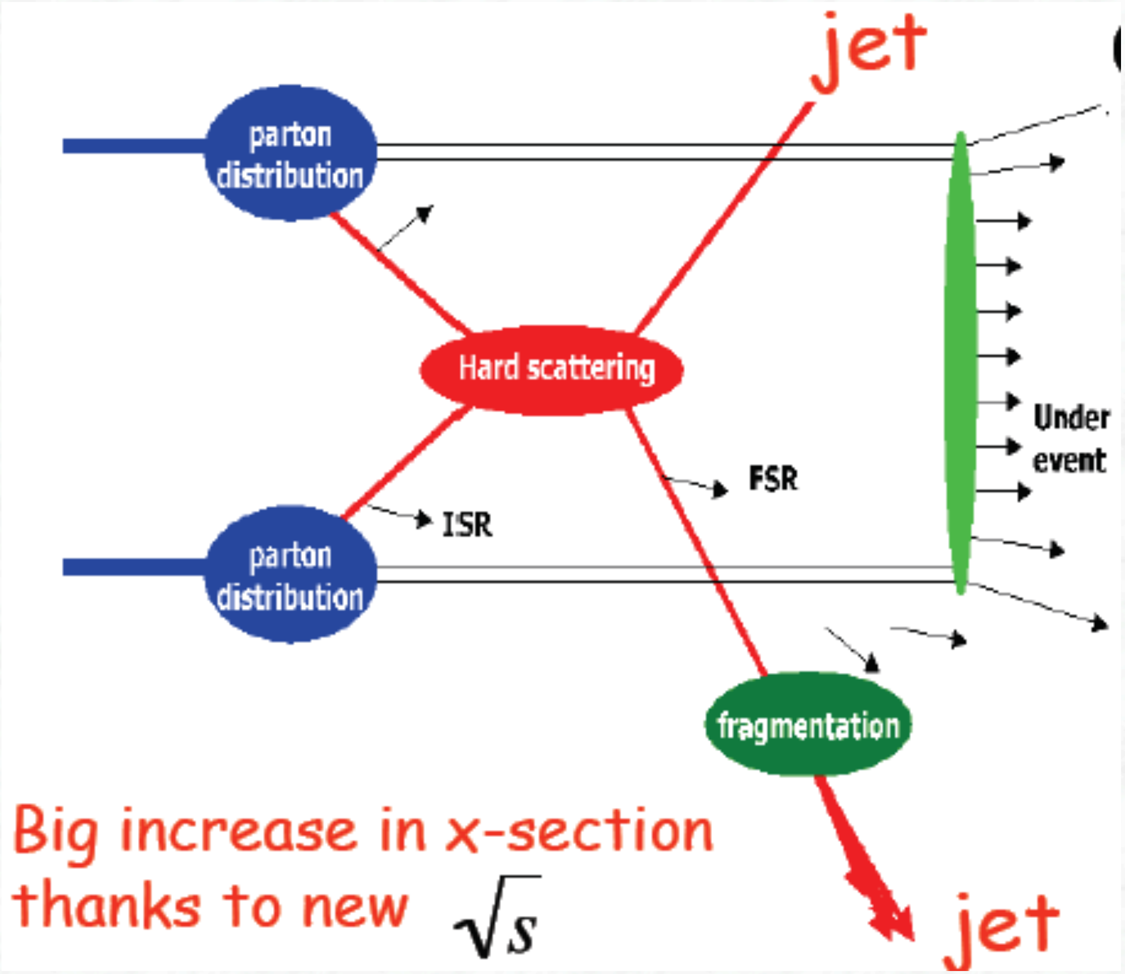

$$\sigma(pp \to A + X) = \sum_{i,j} \int f_{q_i}(x_i, Q^2) f_{q_j}(x_j, Q^2) \sigma(q_i q_j \to A) dx_i dx_j$$

4.2 Hard scattering formalism

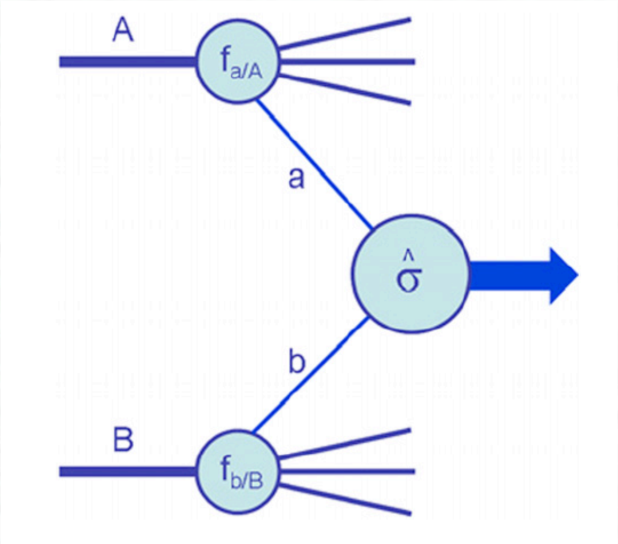

Illustration of a hard proton-proton interaction

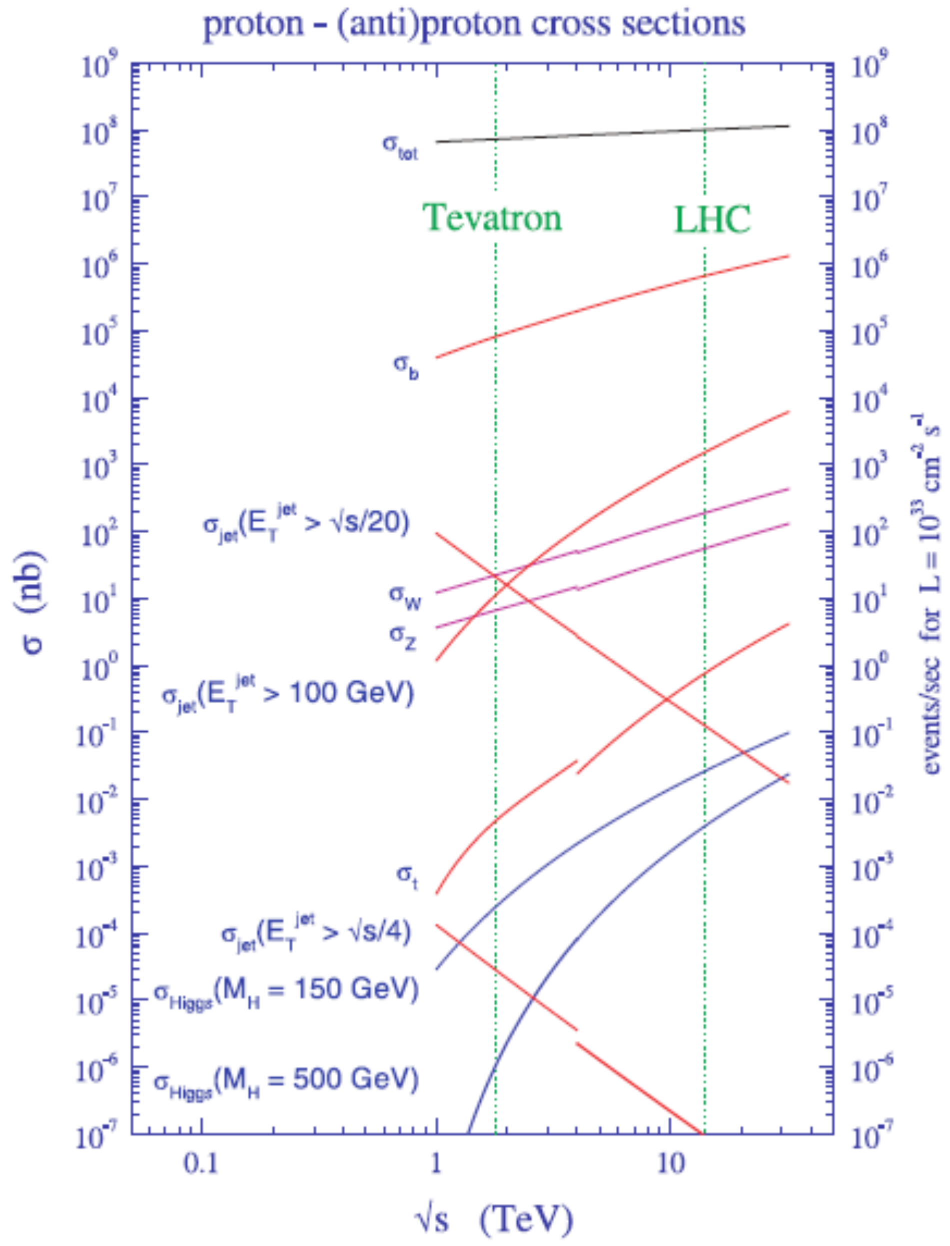

Cross sections for important hard scattering Standard Model processes at the Tevatron and the LHC colliders

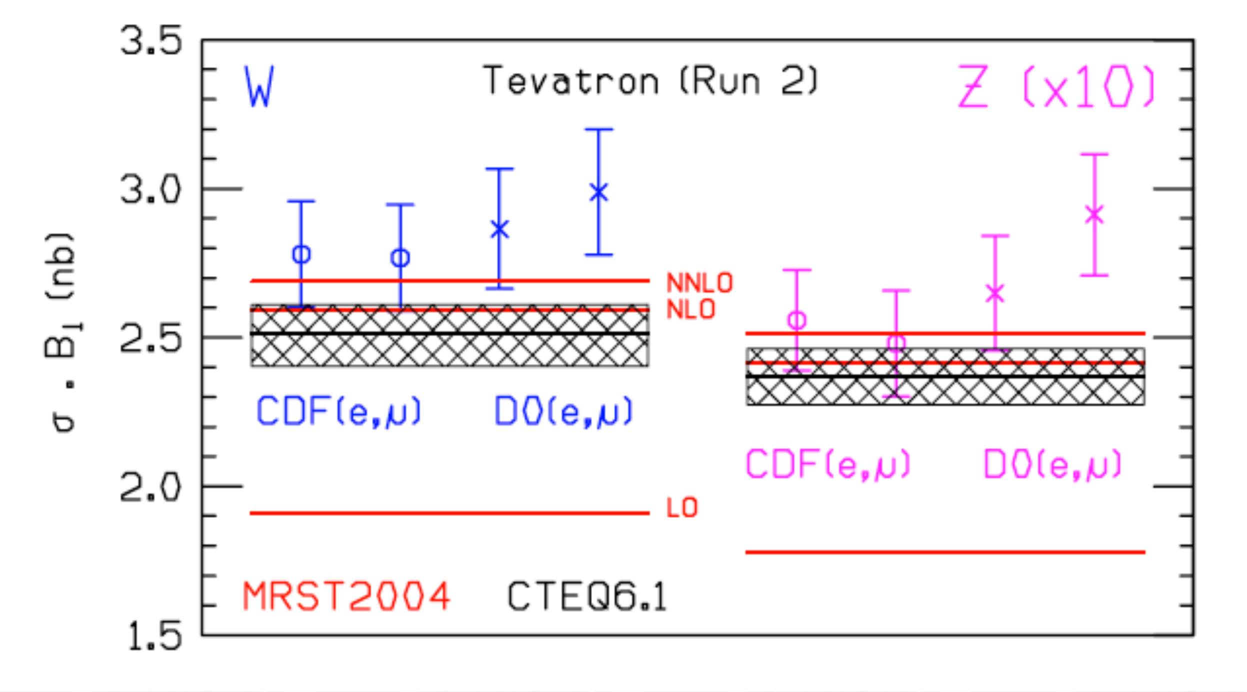

Predictions for the W and Z total cross section at the Tevatron, using MRST2004 and CTEQ6.1 pdfs, compared with measurements from the CDF and D0 experiments. The MRST predictions are shown at LO, NLO and NNLO. The CTEQ6.1 NLO predictions are shown together with the accompanying error band resulting from pdf uncertainties.

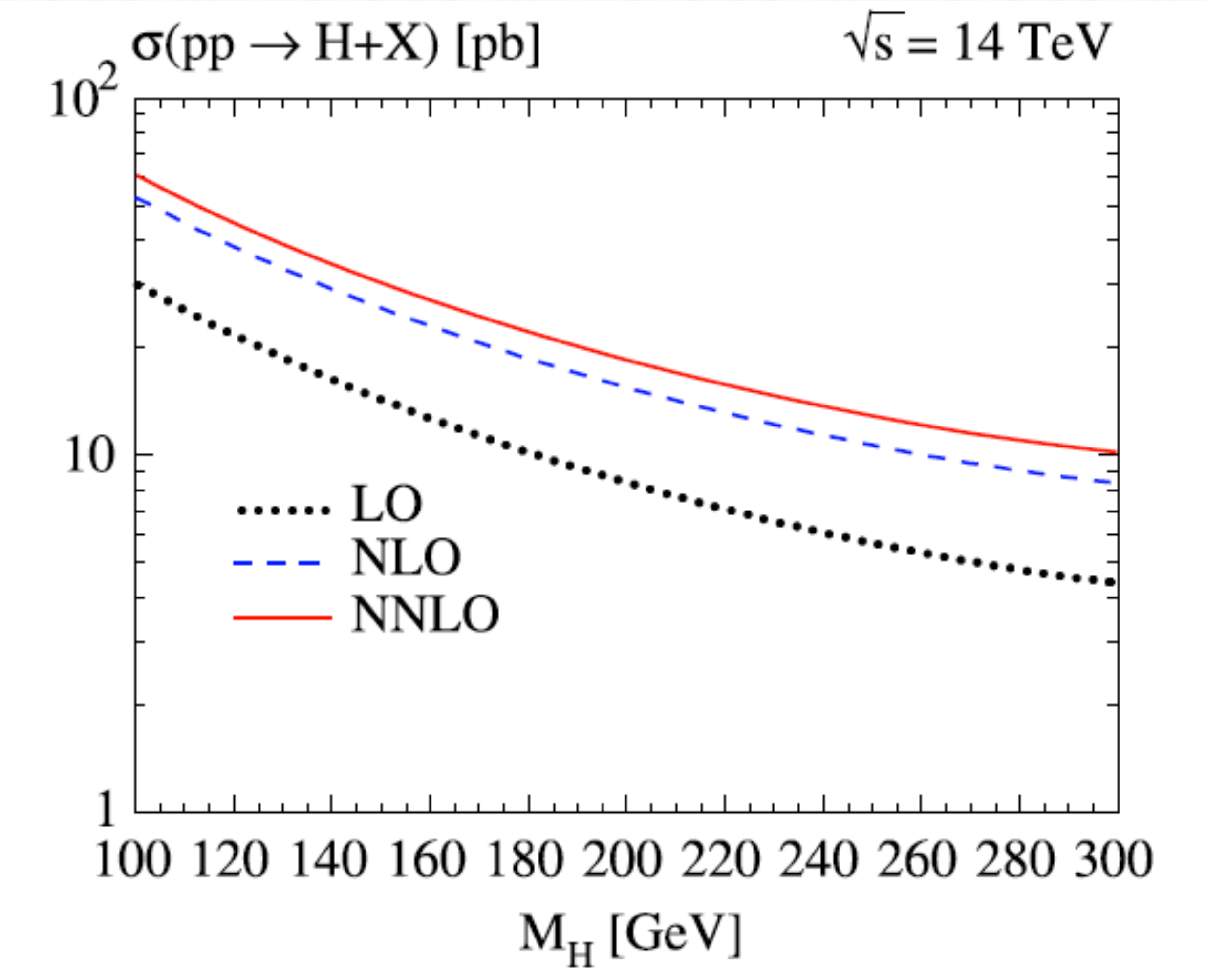

The inclusive Higgs boson production cross section as a function of the Higgs boson mass at LO, NLO and NNLO.

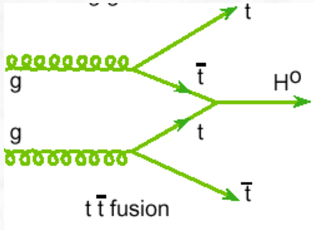

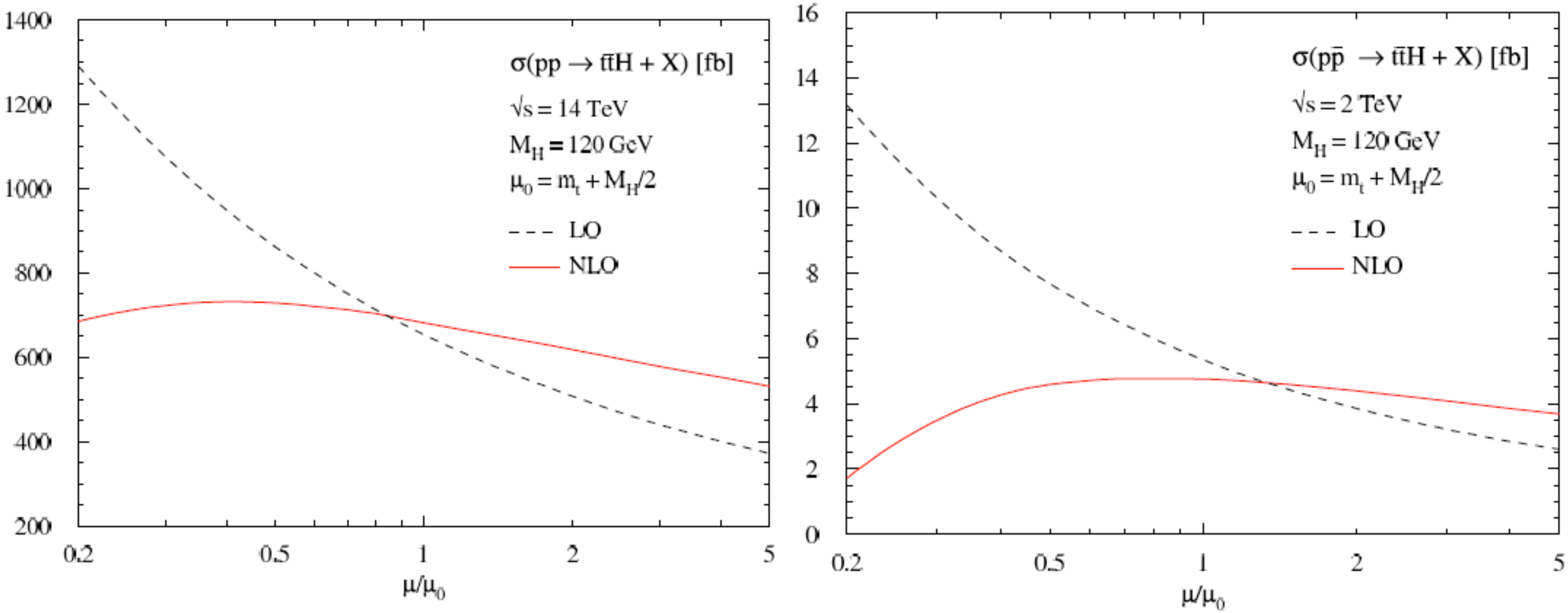

Variation of the ttH production cross section at the LHC 14 TeV pp collider (left) and at the Tevatron 2 TeV ppbar collider (right) with the renormalization and factorization scale $\mu = \mu_R = \mu_F$, varied around the value $\mu_0 = m_t + m_H / 2$.

4.3 Parton Distribution functions (pdf)

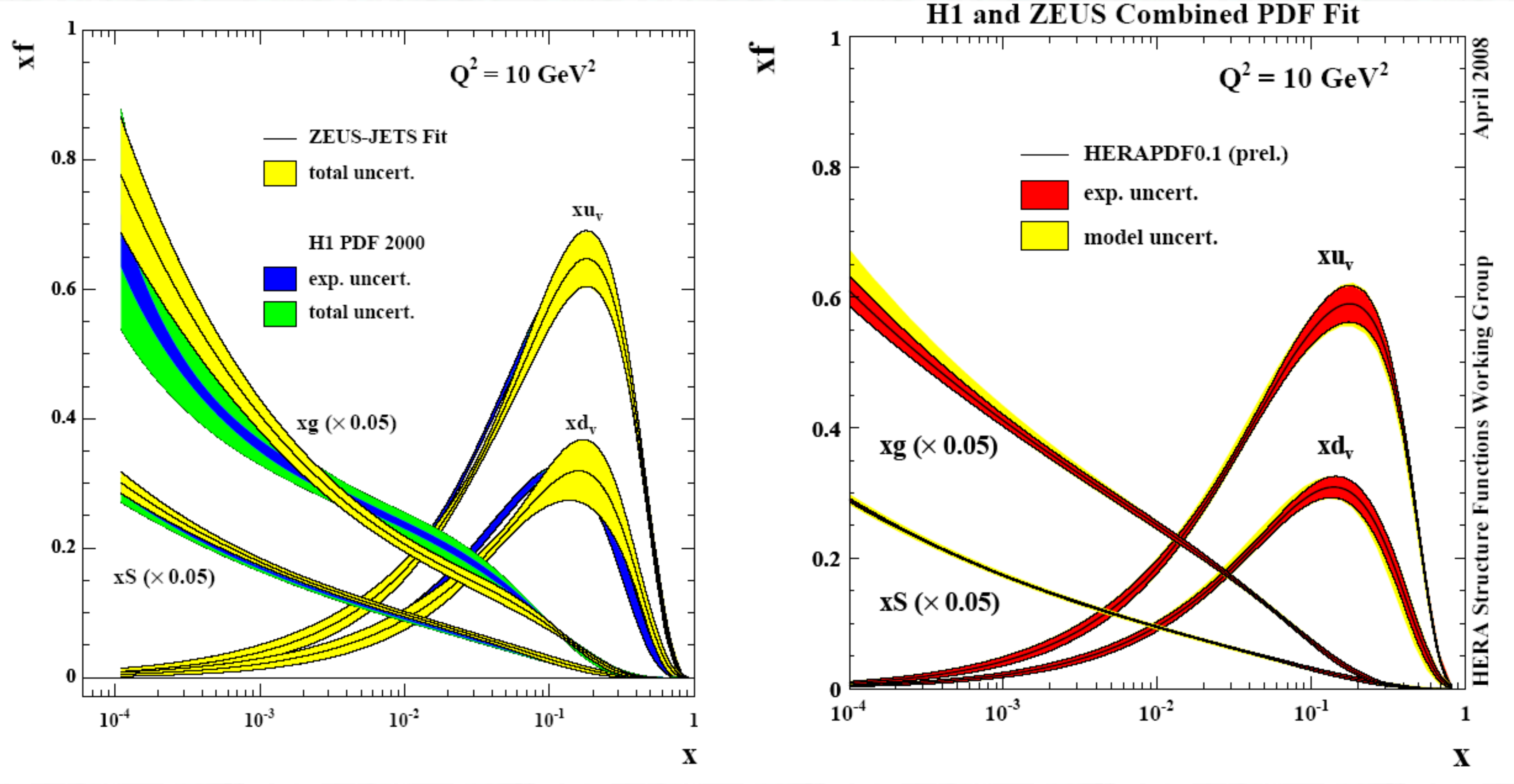

- The measurements of the parton distribution functions is the domain of Deep Inelastic Scattering (DIS) experiments

  (BCDMS, NMC,…, HERA)

- In addition, many processes measured at hadron colliders contribute

Other experimental data:

reaction	subprocess	information
$p\bar{p} \to W + X$	$q\bar{q} \to W$	$u, d, u/d$
$`\nu' N \to \mu^+\mu^- + X$	$\nu s \to \mu c$	s
$pp, pN \to \ell^+\ell^- + X$	$q\bar{q} \to \ell^+\ell^-$	$\bar{d}/\bar{u}$
$hh \to \gamma + X$	$qg \to q\gamma$	g
$p\bar{p} \to \text{jets} + X$	$gg \to gg$ $qg \to qg$ $qq \to qq$	$g, (q)$

History of Deep Inelastic Scattering (DIS) experiments

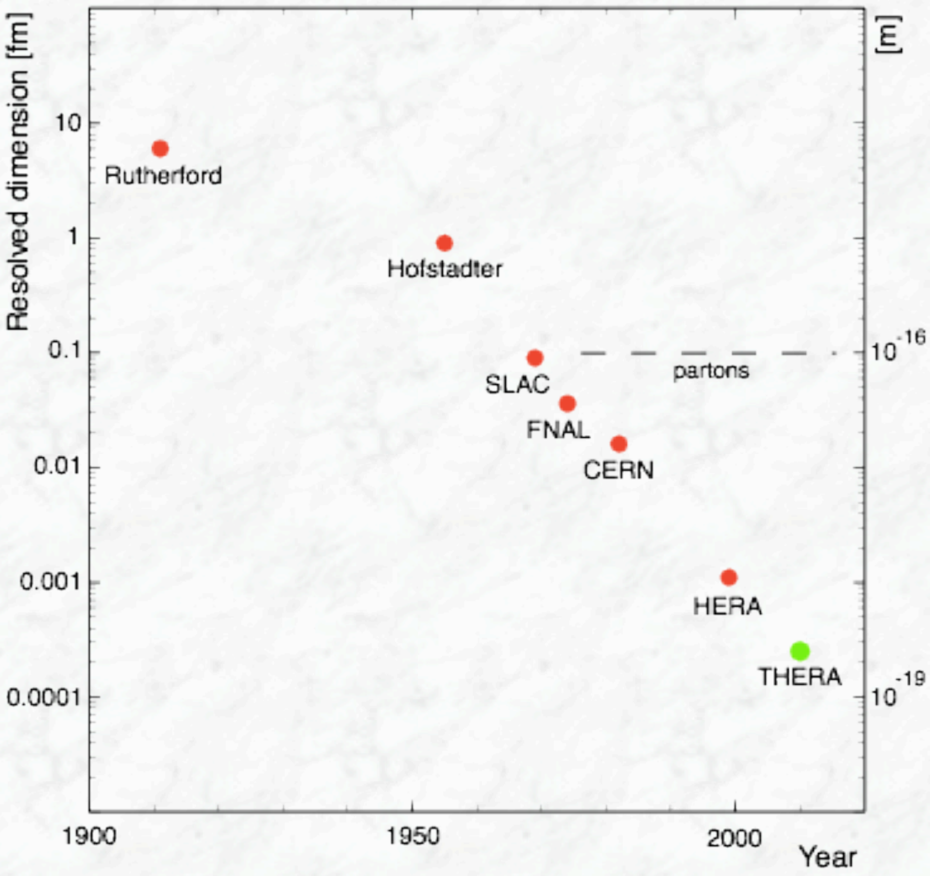

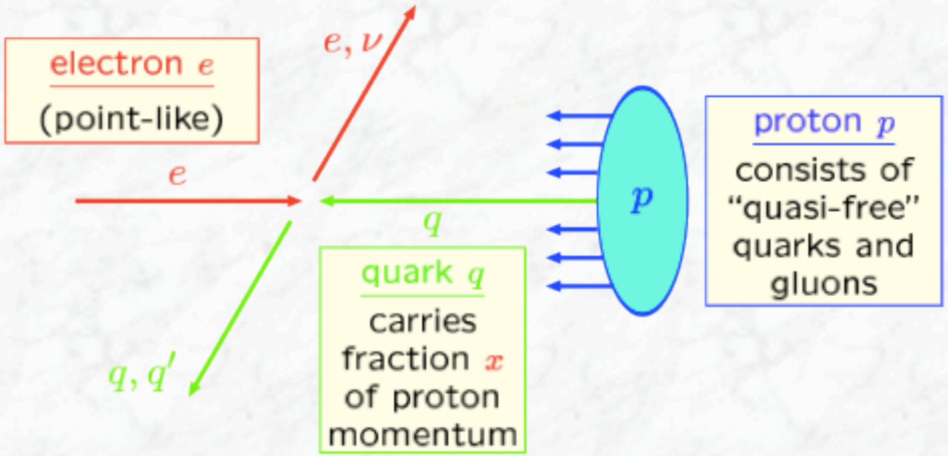

THERA is an idea of an ep collider with a c.m.s. energy of 1 TeV,

e.g. extend the LHC to collide electrons and protons

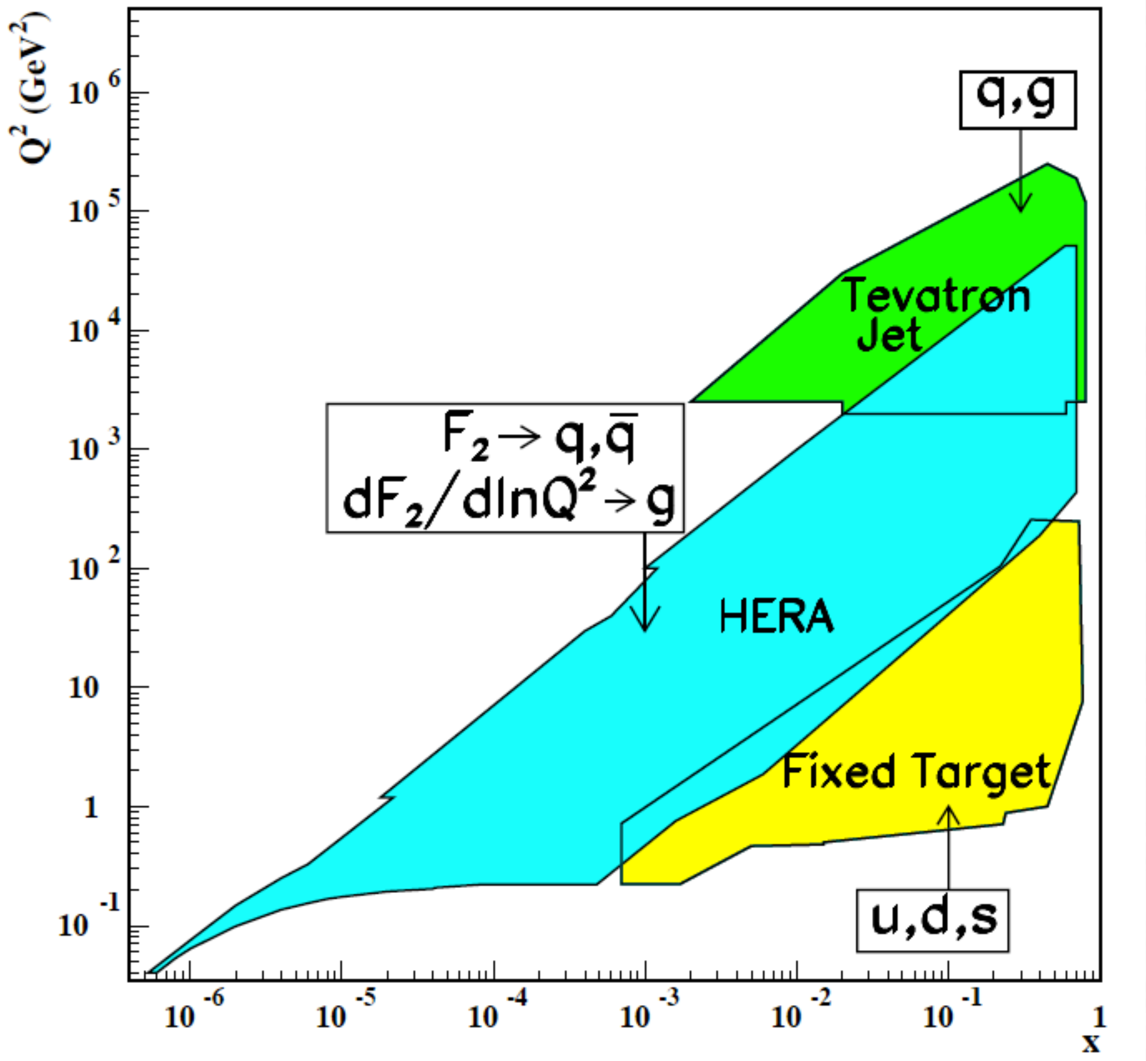

Kinematic domains in x and Q2 probed by fixed-target and collider experiments, shown together with the constraints they make on the various parton distributions (from Particle Data Group).

deep inelastic ep scattering (DIS) =
incoherent sum of elastic eq scattering:

$$\sigma(ep) = \sum_{q,\bar{q} \text{ in } p} f_{q|p} \cdot \sigma(eq)$$

parton distribution $f_{q|p}(x)$:

probability distribution to find a parton of flavor q with momentum fraction x in the proton

$\sigma(eq)$:

differential eq cross section (depends on scattering angle and eq center-of-mass energy)

So, if parton distributions are known, the cross sections can be predicted, or vice versa: from a measurement of the cross sections, the parton distributions can be inferred

Important: Q^2 dependence, QCD effects

DIS Signatures

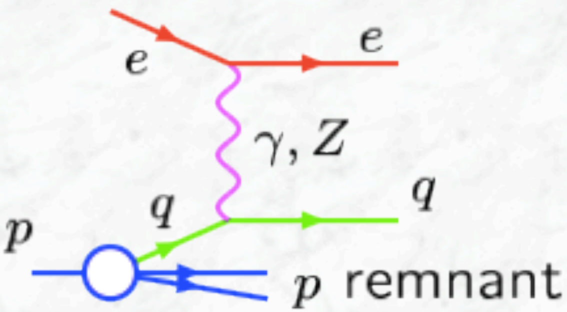

Neutral Current (NC)

- Scattered electron
  $\Rightarrow$ isolated
  $\Rightarrow$ energy $\gtrsim 10\,\text{GeV}$
- One or more "central" jets
- Proton remnant
  energy deposition around beam pipe in p direction

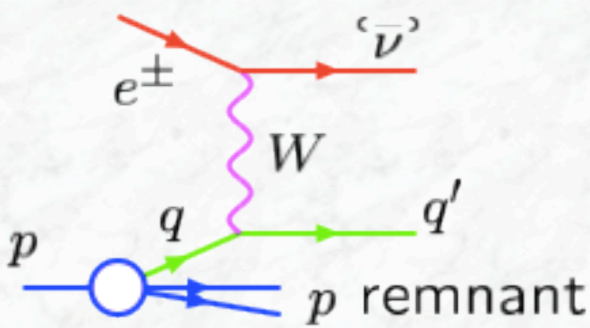

Charged Current (CC)

- Scattered neutrino
  $\Rightarrow$ invisible
  $\Rightarrow$ causes missing transverse momentum
- Hadronic final state
  $\Rightarrow$ as in NC reactions

NC and CC cross sections

Measurements of $d\sigma/dQ^2$ at HERA:

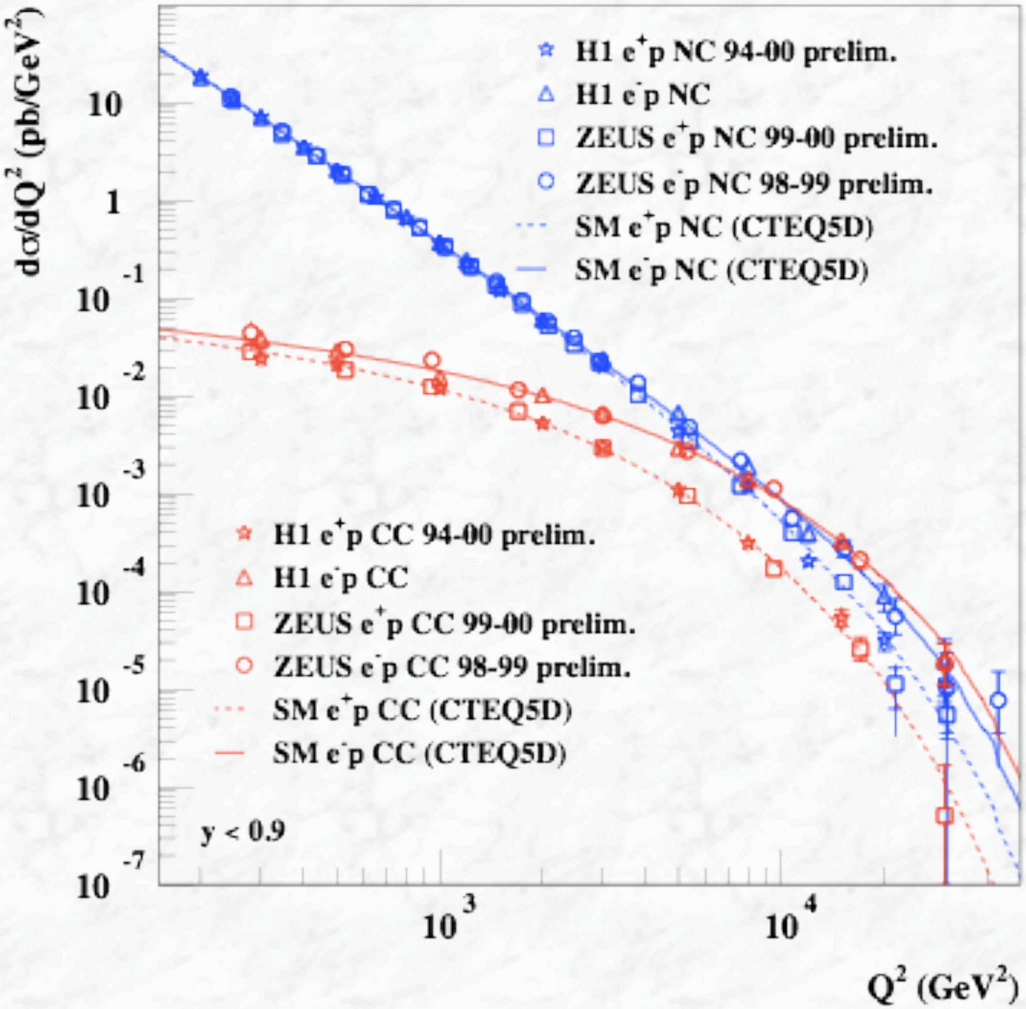

- HERA: first simulteneous measurements of NC and CC reactions, e^+p und e^-p in the same experiment.
- For $Q^2 \gtrsim M^2_{W,Z}$ we have $d\sigma/dQ^2(\mathrm{NC}) \sim d\sigma dQ^2(\mathrm{CC})$ (electroweak unification).
- Cross sections vary by many orders of magnitude, measurements still statistics-dominated at high Q^2.

Quark Parton Model (QPM) cross sections

The ep cross section

$$\frac{d^2\sigma_{NC}(e^\pm p)}{dx\,dQ^2} = \frac{2\pi\alpha^2}{Q^4}\left(Y_+ F_2^{NC} \mp Y_- x F_3^{NC}\right)$$

$$\frac{d^2\sigma_{CC}(e^\pm p)}{dx\,dQ^2} = \frac{\pi\alpha^2}{8\sin^4\theta_W}\frac{1}{(Q^2+M_W^2)^2}\times \left(Y_+ F_2^{CC\pm} \mp Y_- x F_3^{CC\pm}\right)$$

$$Y_\pm = 1 \mp [1-y)^2$$

- $F_{2,3} = F_{2,3}(x,Q^2)$ = structure functions
- xF_3 terms violate parity.
- Representation of the DIS cross section in terms of structure functions does not require knowledge of partons.
- Approximation: longitudinal structure function $F_L \approx 0 \Rightarrow F_2 = 2xF_1$ (Callan–Cross relation, ony valid if partons carry spin 1/2).

QPM cross section (cont.)

Structure functions and PDFs

Calculate $d\hat{\sigma}/dQ^2$ and insert in (*)
⇒ relation between structure fnct's and PDFs:

NC:

$$F_2^{NC} = x \sum_{q=d,u,s,c,b} A_q(Q^2)\ [q+\bar{q}]$$

$$xF_3^{NC} = x \sum_{q=d,u,s,c,b} B_q(Q^2)\ [q-\bar{q}]$$

$$A_q(Q^2) = Q_q^2 - 2Q_q v_e v_q\, P_Z + (v_e^2+a_e^2)(v_q^2+a_q^2)\, P_Z^2$$

$$B_q(Q^2) = -2Q_q a_e a_q\, P_Z + 4 v_e a_e v_q a_q\, P_Z^2$$

$$P_Z = \frac{Q^2}{Q^2+M_Z^2}$$

- t quarks do not contribute to NC reactions at HERA ($2m_t \approx 350$ GeV $> \sqrt{s}$)
- Phase space suppression of c and b quarks in final state is negligible
- Mass effects of c and b quarks in initial state are absorbed in PDFs

CC:

$$F_2^{CC+}, xF_3^{CC+} = \sum_{q=d,s} xq \pm \sum_{q=u,c} x\bar{q}$$

$$F_2^{CC-}, xF_3^{CC-} = \sum_{q=u,c} xq \pm \sum_{q=d,s} x\bar{q}$$

- b and t contributions are neglected (large m_t and small CKMM elements V_{i3})

The principle of the pdf determination

- The parton distribution functions cannot be described from first principles. A parametrization is performed at a reference scale Q_0 as a function of x

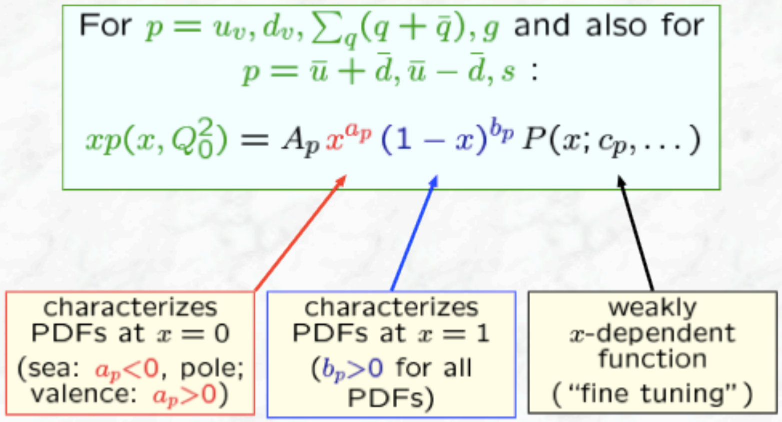

- The QCD evolution (DGLAP) is used to calculate the pdfs at a higher Q^2 scale (up to NLO, partly NNLO precision)

- Predictions for experimental observables (cross sections, structure functions, …) are calculated

- pdf parameters are determined from a X^2 fit to the experimental data

- Fits are performed by several groups: CTEQ, MRST, ….

The QCD evolution equations

DGLAP equations:

(Dokshitzer, Gribov, Lipatov, Altarelli, Parisi)

$$\frac{\mathrm{d}}{\mathrm{d}\ln Q^2}\begin{pmatrix} q^{\mathrm{S}} \\ q^{\mathrm{NS}} \\ g \end{pmatrix} = \frac{\alpha_s}{2\pi}\begin{pmatrix} P_{qq} & 0 & P_{qg} \\ 0 & P_{qq} & 0 \\ P_{gq} & 0 & P_{gg} \end{pmatrix} \otimes \begin{pmatrix} q^{\mathrm{S}} \\ q^{\mathrm{NS}} \\ g \end{pmatrix}$$

$$P_{ba} \otimes q(x, Q^2) \equiv \int_x^1 \frac{\mathrm{d}\xi}{\xi}\, q(\xi, Q^2)\, P_{ba}\left(\frac{x}{\xi}\right)$$

P_{ba} = QCD splitting function
$\propto |\mathrm{ME}|^2$ for $a(\xi) \to b(x)$

$$q^{\mathrm{S}}(x, Q^2) = \sum_q \left[q(x, Q^2) + \bar{q}(x, Q^2)\right]$$

= singlet PDF

$$q^{\mathrm{NS}}(x, Q^2) = q_i(x, Q^2) - \bar{q}_i(x, Q^2) \quad \text{or}$$
$$q_i(x, Q^2) - q_j(x, Q^2)\ (i \neq j)$$

= non-singlet PDF
(e.g. $d_v, u_v =$ valence quark PDFs)

Leading-log approximation (LLA)

- splitting functions in leading order α_s
- QPM formulae remain valid if the PDFs are solutions of the DGLAP equations

Next-to-leading-log approximation (NLLA)

- P_{ba} in next-to-leading order (α_s^2)
- additive corrections to structure functions (in particular $F_L \neq 0$)
- used in HERA analyses

scaling violations via QCD effects

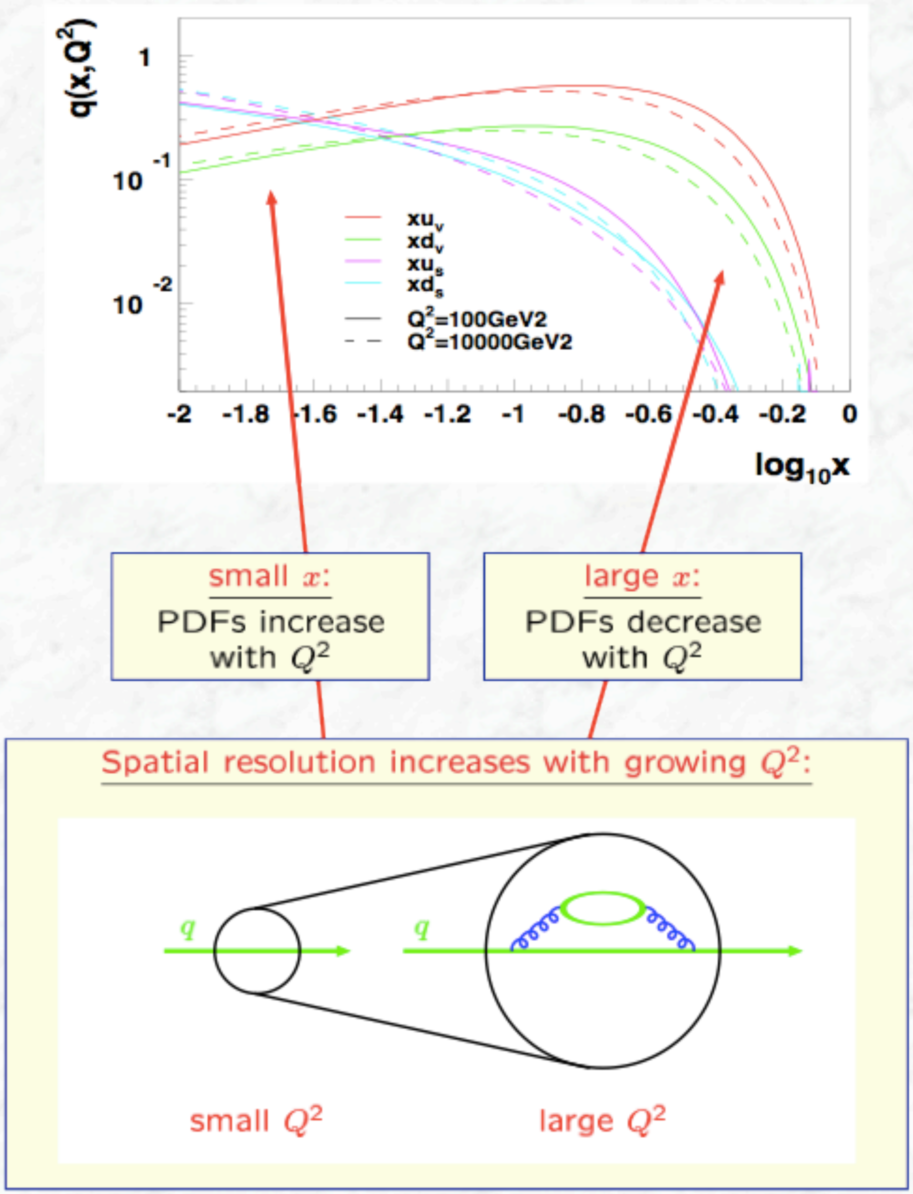

The legacy of HERA

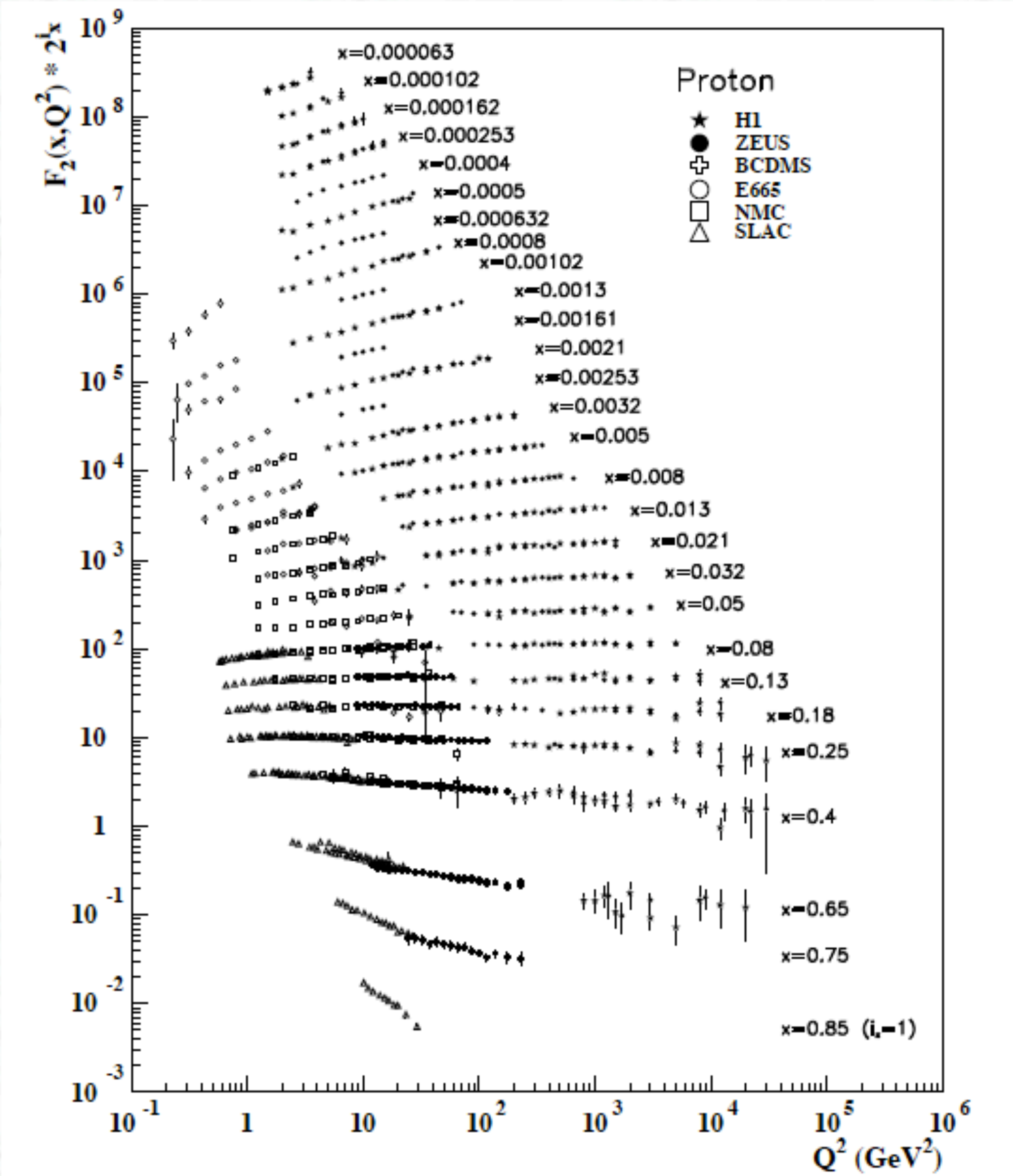

An enormous extension of the kinematic range both to high Q^2 and to low x

- low x: significant constraints on the gluon
- high Q^2: W/Z exchange and probe of the electroweak sector.

QCD fits to data

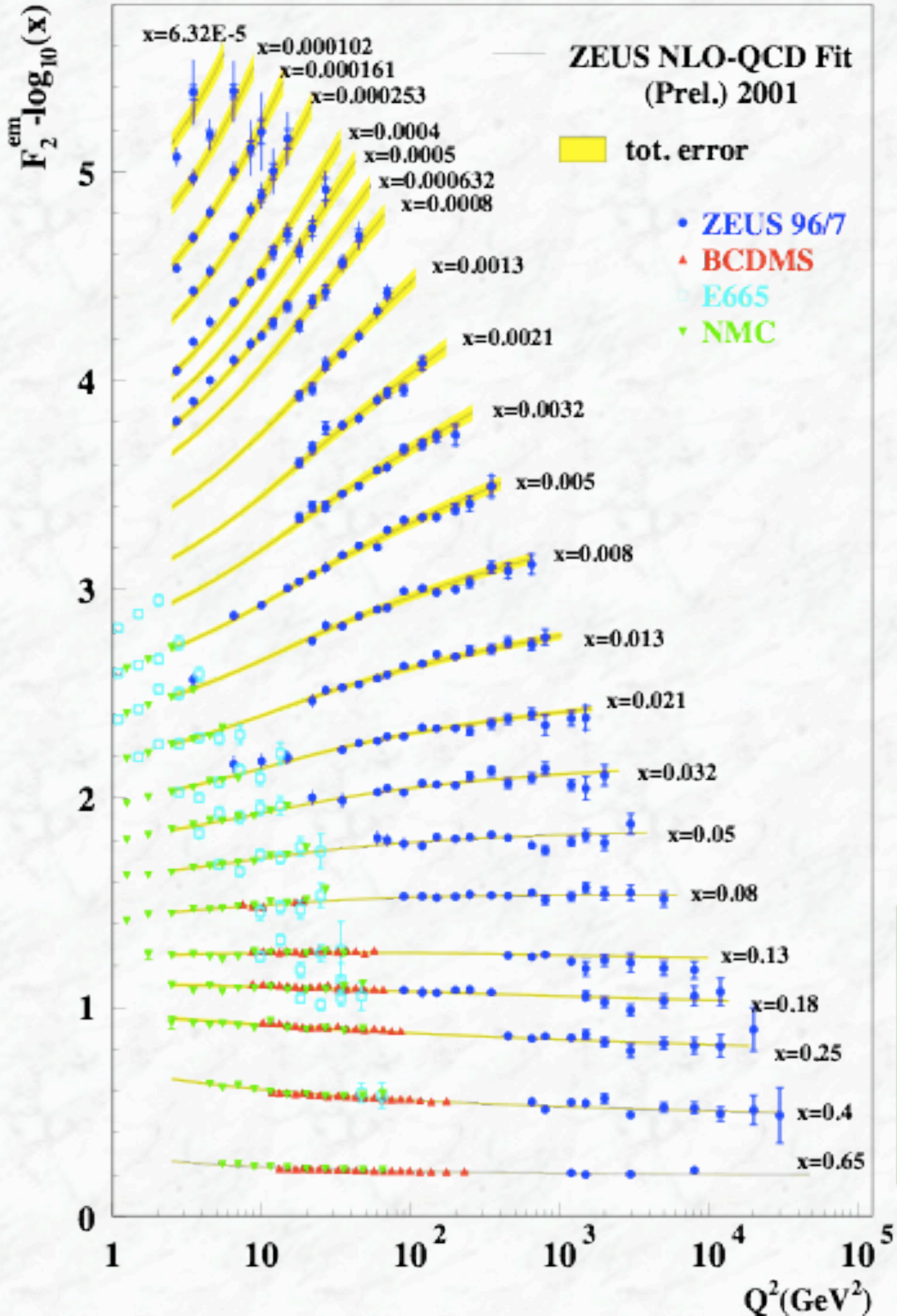

NC and CC DIS data

- Fixed target experiments: measurements of structure functions (different target nuclei)
  NC: BCDMS, NMC, E665, SLAC,. . .
  CC: CCFR, CDHS(W), CHARM, BEBC, . . .
- Structure functions and cross sections from ZEUS and H1

Impact of HERA data on the LHC: W/Z production as an example

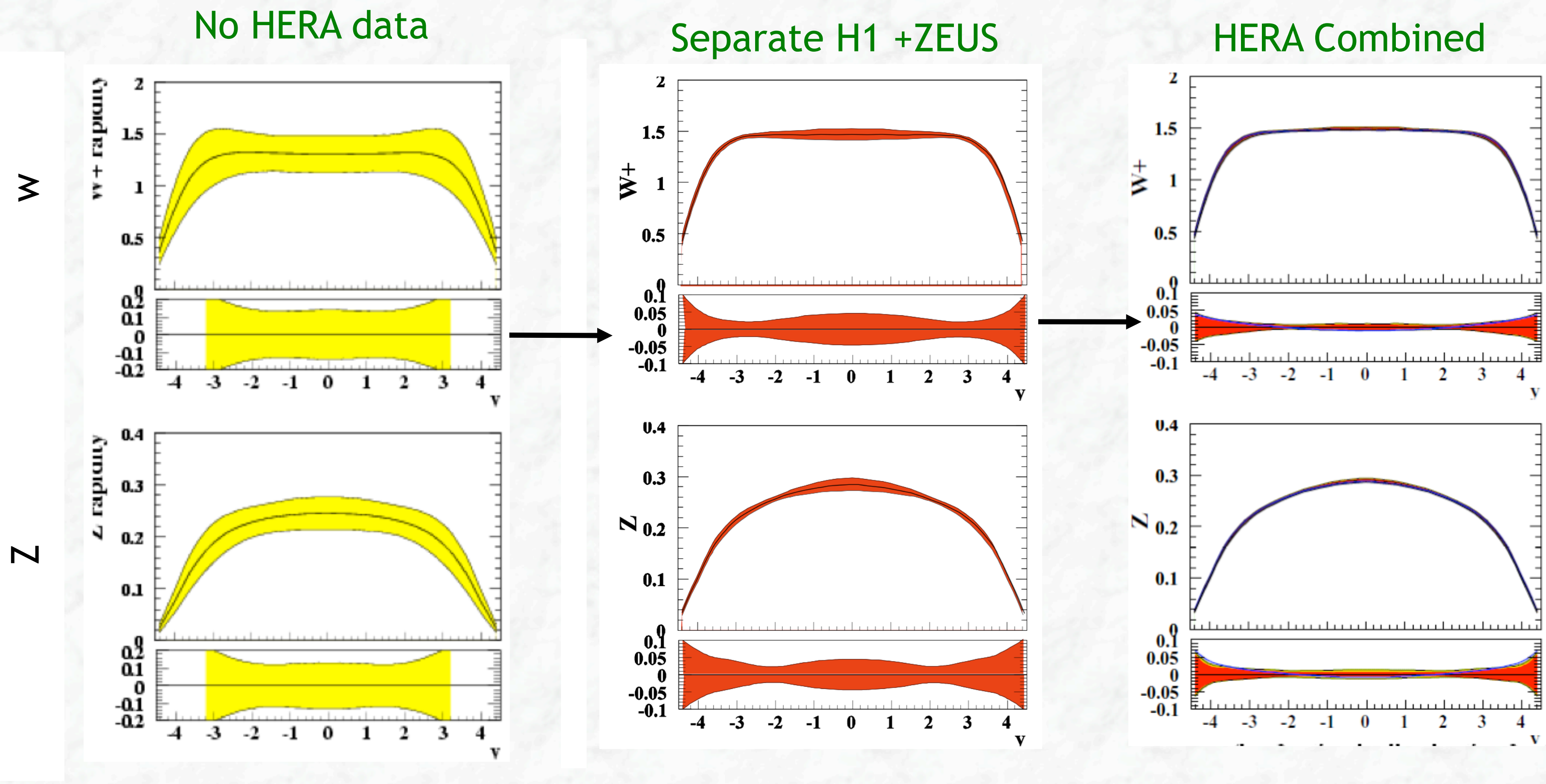

W and Z production cross sections and rapidity distributions are much more precisely known
(mainly due to better constrained low-x region (gluons), due to gq → Wq and g → qqbar splitting contributions producing the necessary antiquarks (sea))

Parton distribution functions (2010)

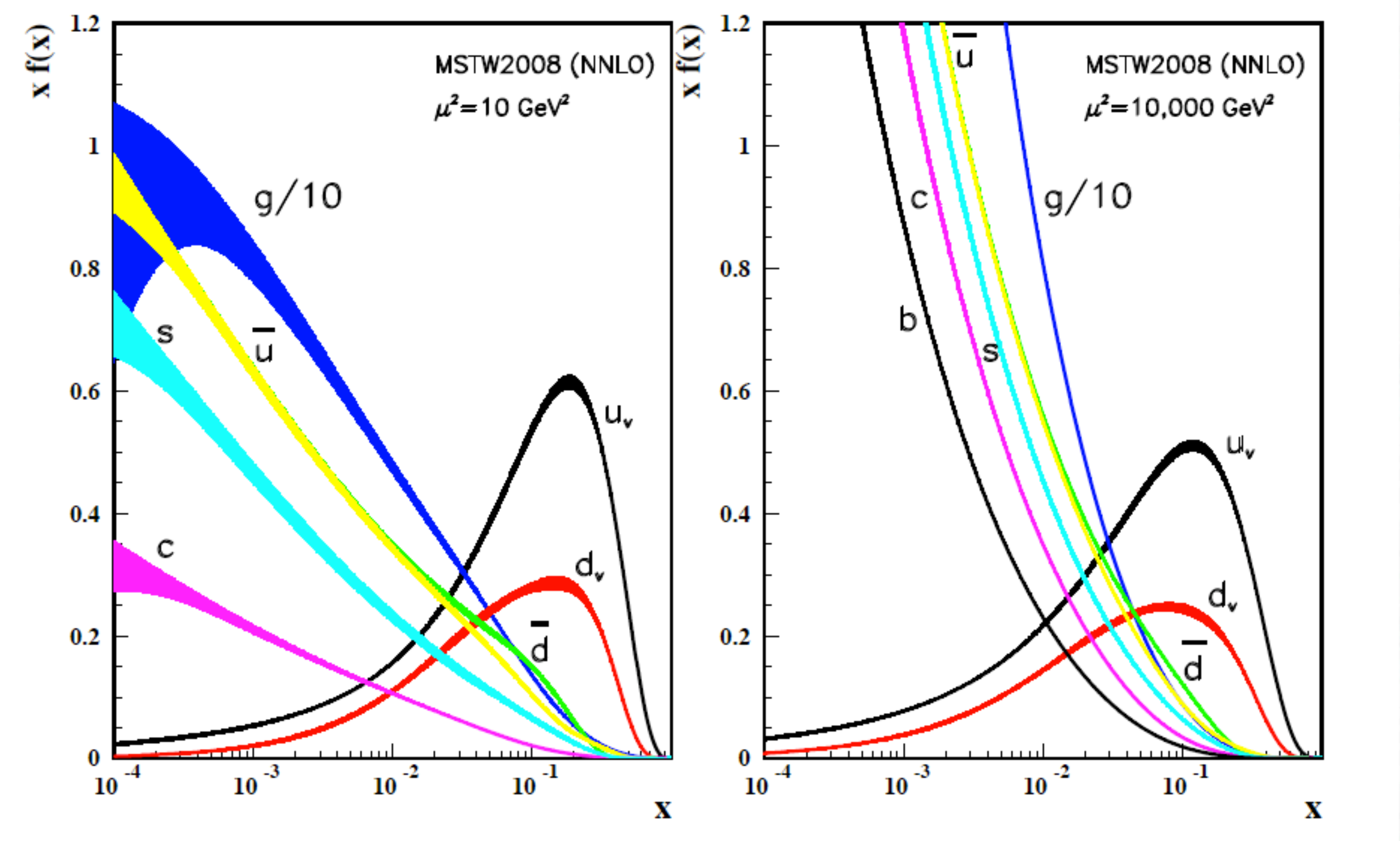

Distributions of x times the unpolarized parton distributions f(x), where f = u_v, d_v, ubar, dbar, s, b, g and their associated uncertainties using the NNLO MRST2006 parametrization at a scale μ^2 = 20 GeV^2 and μ^2 = 10.000 GeV^2.

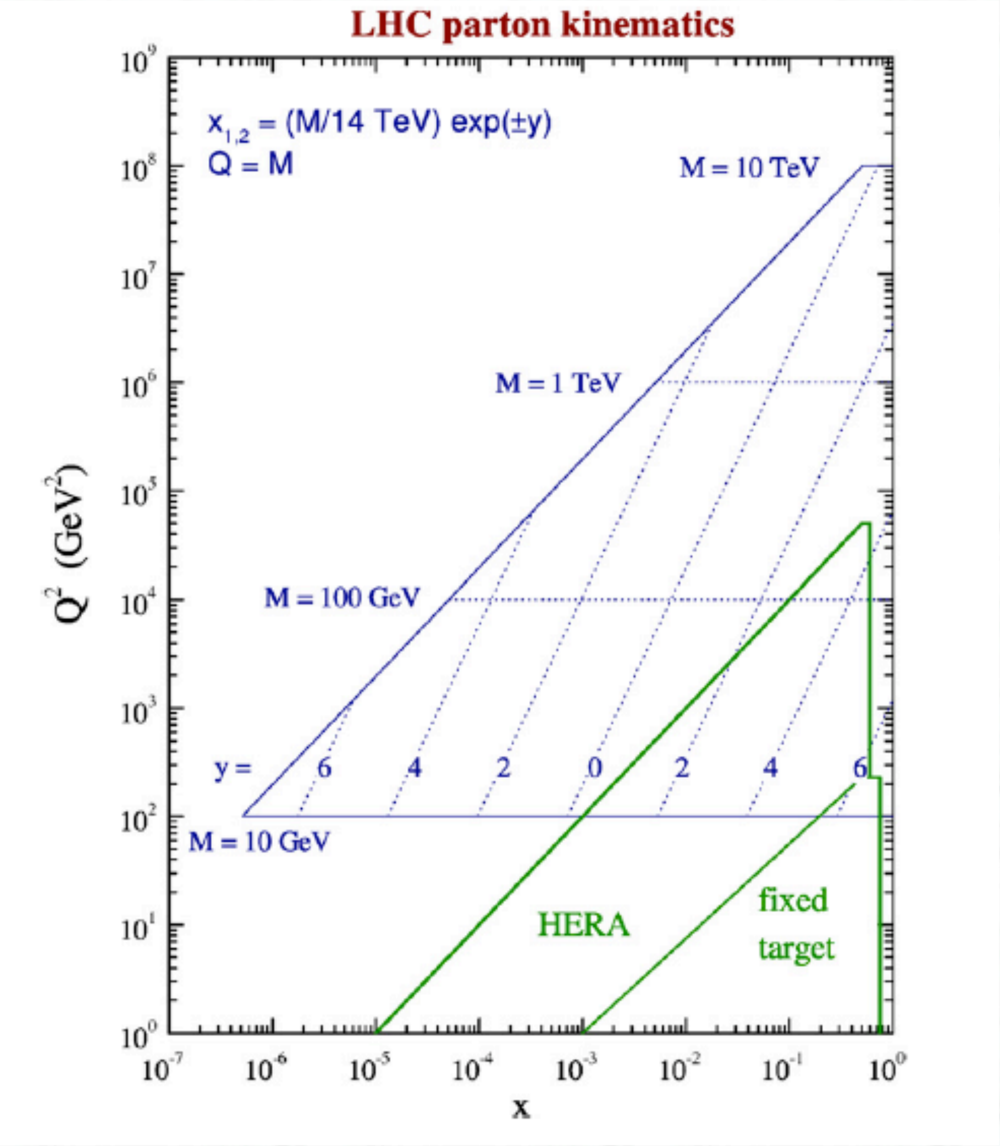

Graphical representation of the relationship between parton (x, Q^2) variables and the kinematic variables corresponding to a final state of mass M with rapidity y at the LHC with $\sqrt{s}$ = 14 TeV

Comparison between the Tevatron and the LHC (14 TeV)

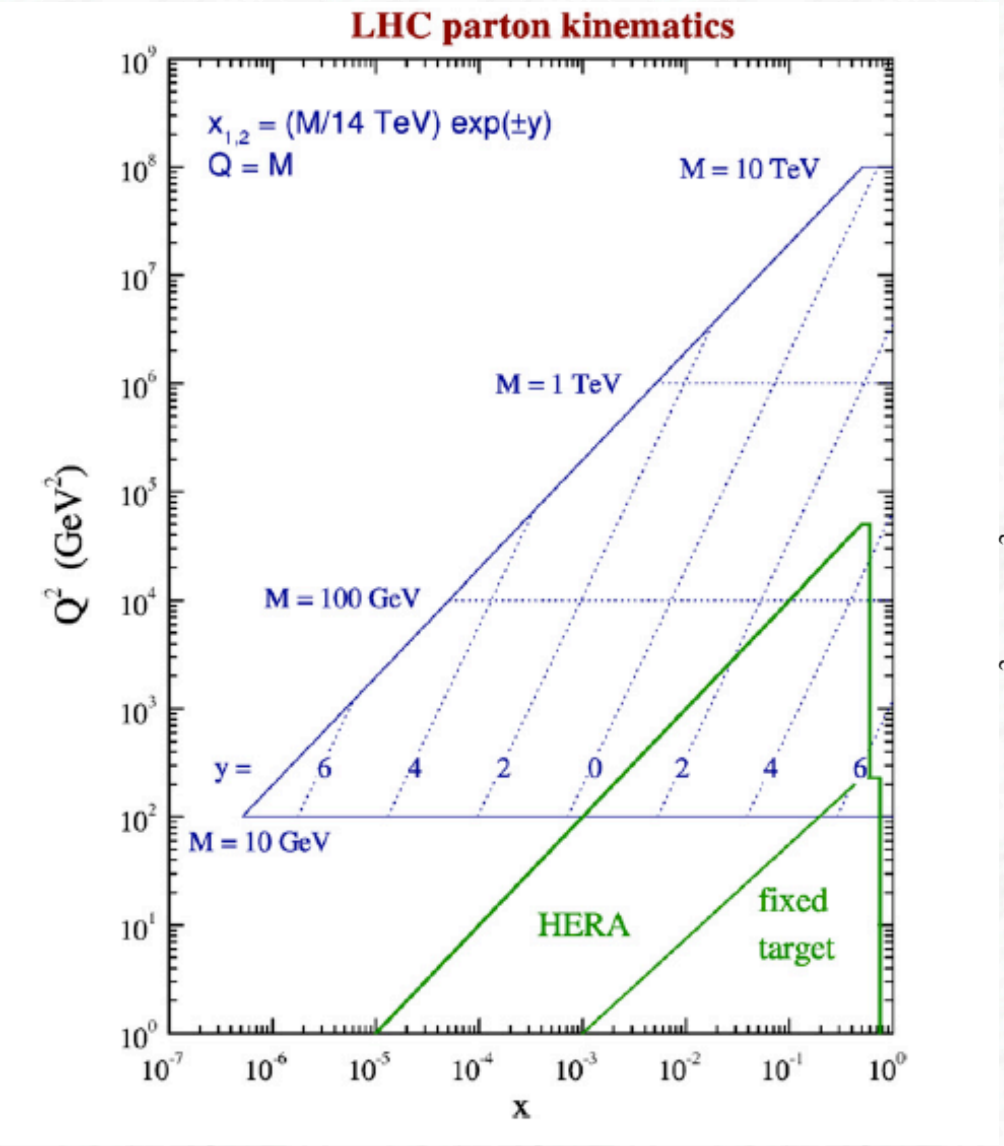

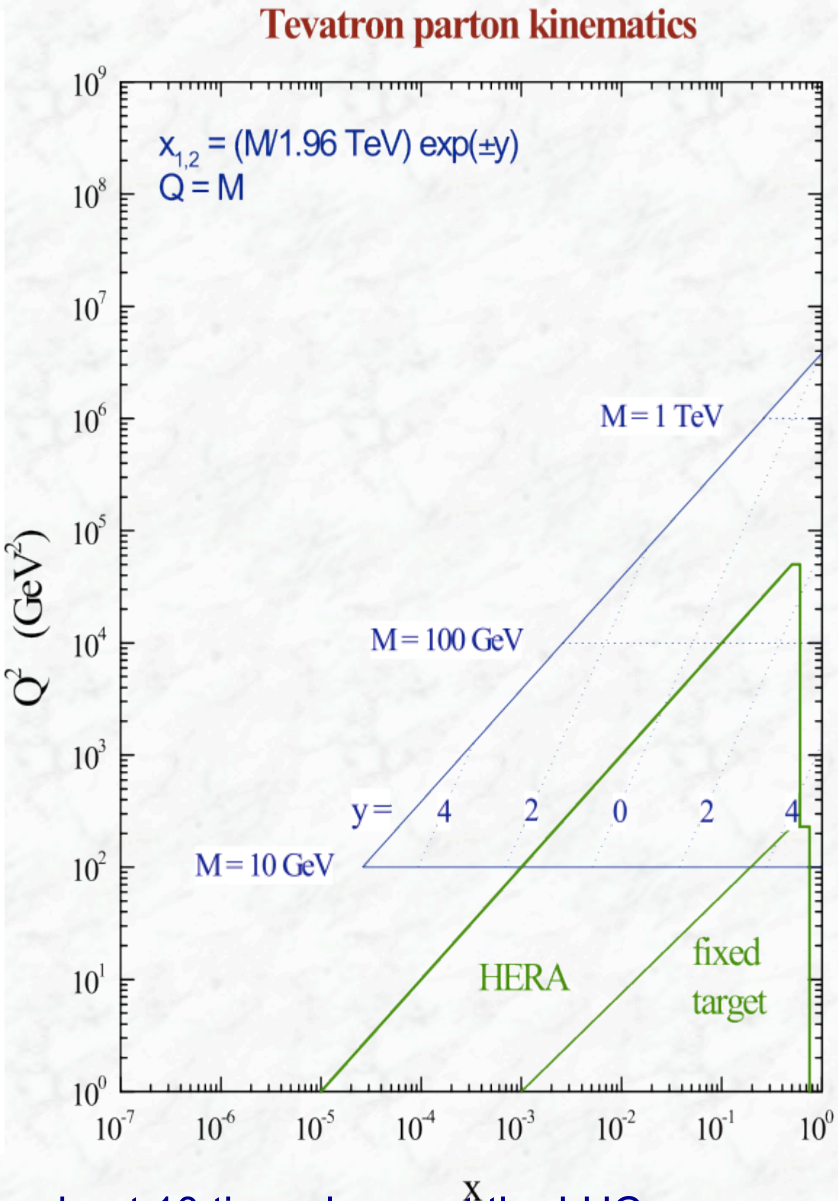

For the same masses (e.g. 100 GeV): x-values about 10 times lower at the LHC

4.4 Soft proton-proton interactions

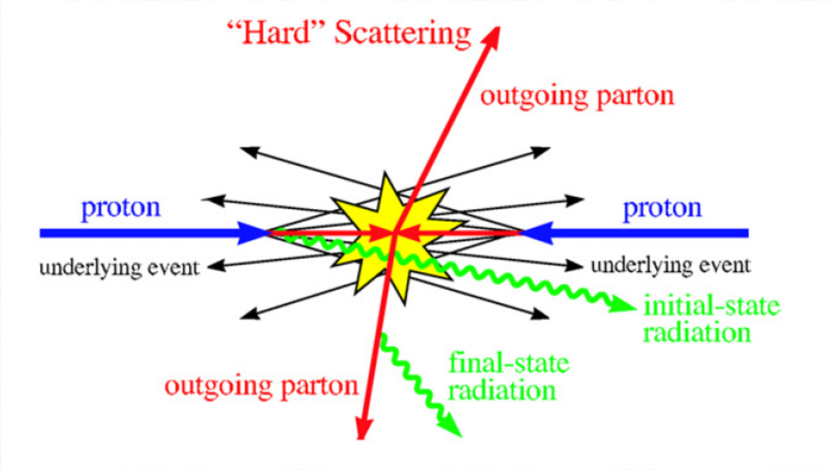

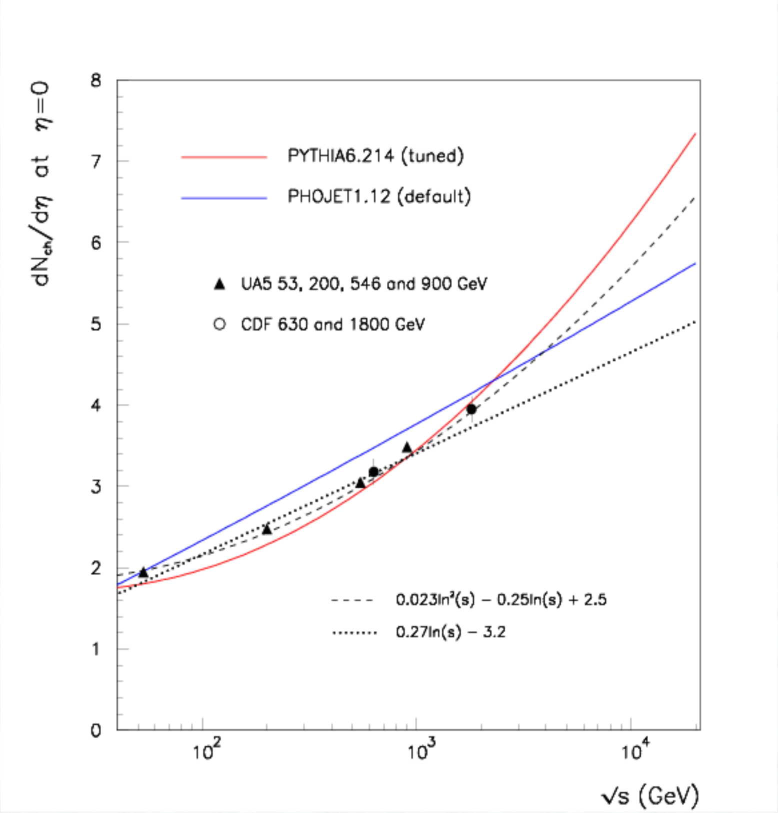

- First physics at the LHC was dominated by large cross section of inelastic hadronic interactions

- Measurements necessary to constrain phenomenological models of soft-hadronic interactions and to predict properties at higher centre-of-mass energies (underlying event, pile-up of minimum bias events at high luminosity, ….)

Inelastic low - p_T pp collisions

Most interactions are due to interactions at large distance between incoming protons
→ small momentum transfer, particles in the final state have large longitudinal, but small transverse momentum

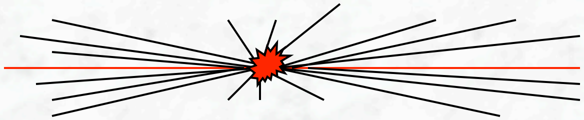

$< p_T > \approx 600$ MeV (of charged particles in the final state)

$$\frac{dN}{d\eta} \approx 7$$

- about 7 charged particles per unit of pseudorapidity in the central region of the detector
- uniformly distributed in ϕ

These events are usually referred to as
"minimum bias events"

(more precise definition follows)

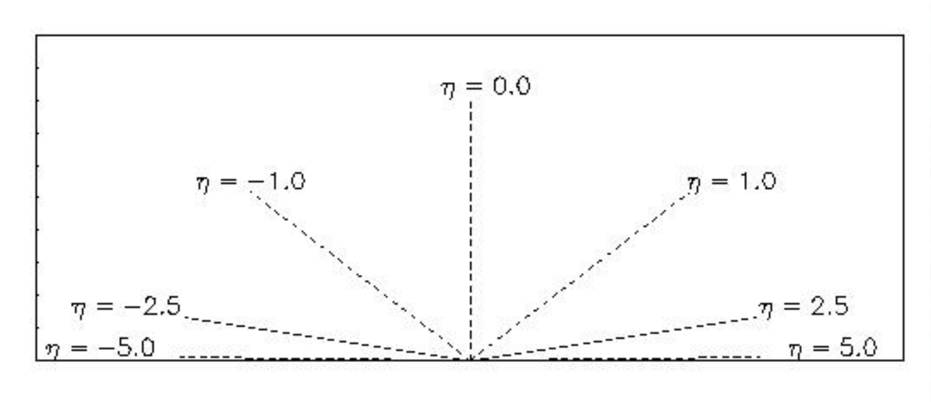

Total inelastic pp cross section

- The total inelastic pp cross section has several components:

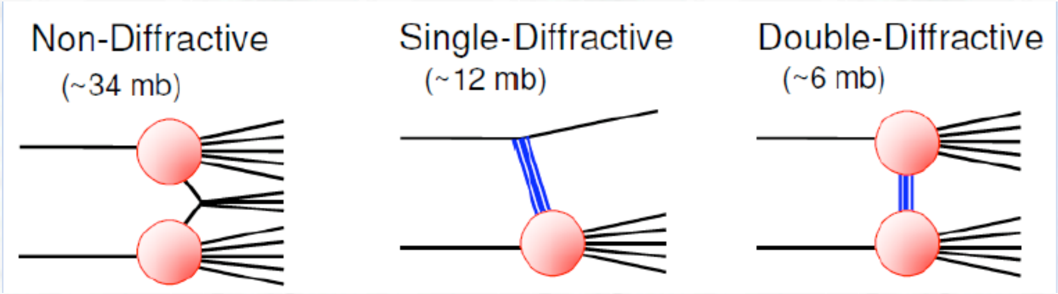

Single **D**iffractive
Double **D**iffractive
Non **D**iffractive

- Use "minimum bias trigger" to study inelastic collisions

(an "experimental definition")

- Different definitions can be found in the literature / previous studies:

(i) Inelastic, non-single diffractive (NSD)

Trigger selection via double-arm coincidence trigger
Removal of remaining single-diffractive component, model dependent

(ii) Inelastic, non-diffractive

Removal of single- and double-diffractive components, model dependent

(iii) Inclusive inelastic

Selection via a single-arm trigger, overlapping with the acceptance of the tracking volume

Soft pp collisions

pp collisions at $\sqrt{s}$ = 14TeV	PYTHIA6.323	PHOJET1.12
σ_{tot}	101.5 mb	119.1 mb
σ_{elas}	22.2 mb	34.5mb
$2^*\sigma_{SD}$	14.4mb	11.0mb
σ_{DD}	10.3mb	4.1mb
σ_{ND}	54.7mb	69.5mb

Minimum bias
Made up of
combination of
non-diffractive
and diffractive

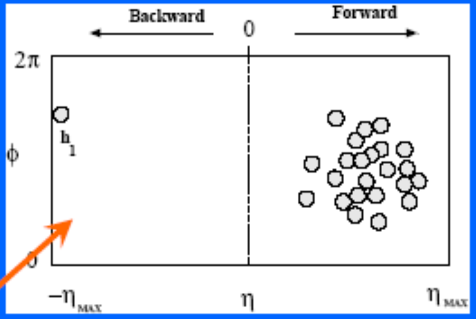

Single diffractive SD

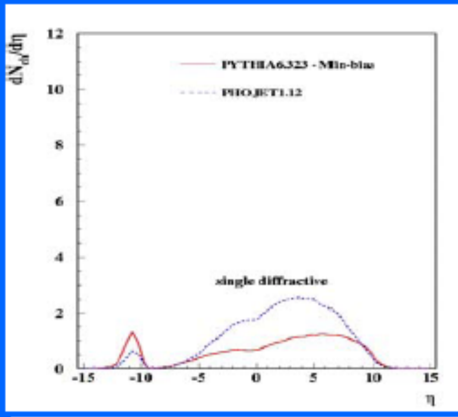

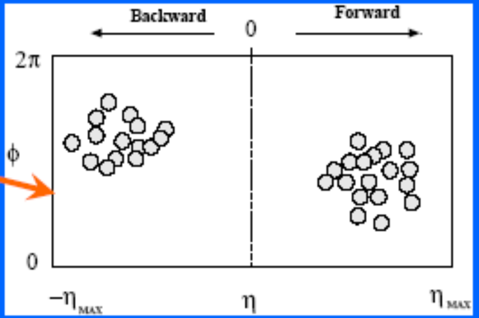

Double diffractive DD

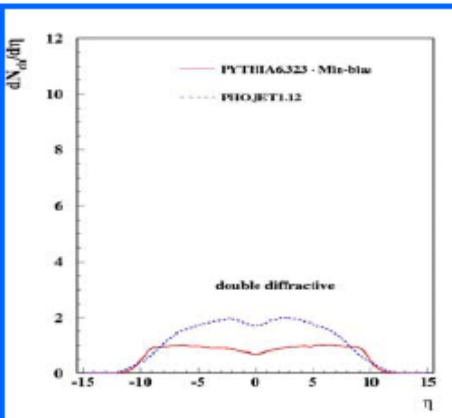

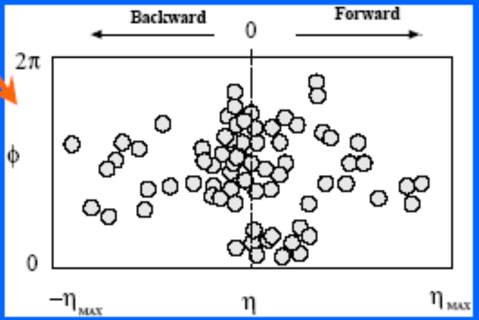

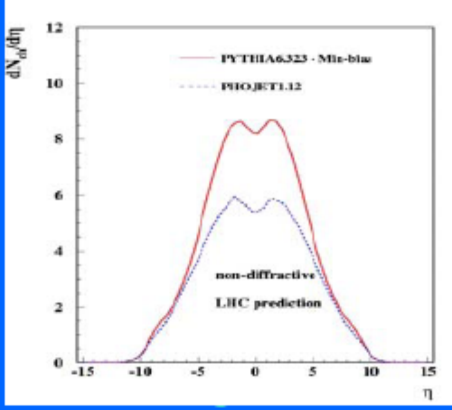

Non-diffractive ND

"Minimum bias events"

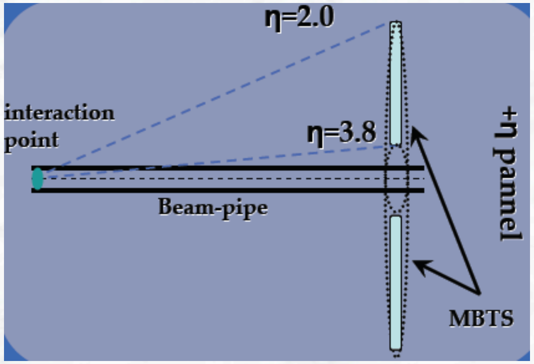

- Minimum bias is an experimental definition, defined by experimental trigger selection and analysis

- Relation to Physics:

$$\sigma_{measured} = f_{sd}\,\sigma_{sd} + f_{dd}\,\sigma_{dd} + f_{nd\text{-}inelestic}\,\sigma_{nd\text{-}inelastic}$$

where f_i are the efficiencies for different physics processes determined by the trigger

NB: need to understand what is measured to allow comparison to previous results, often presented for non-single diffractive events

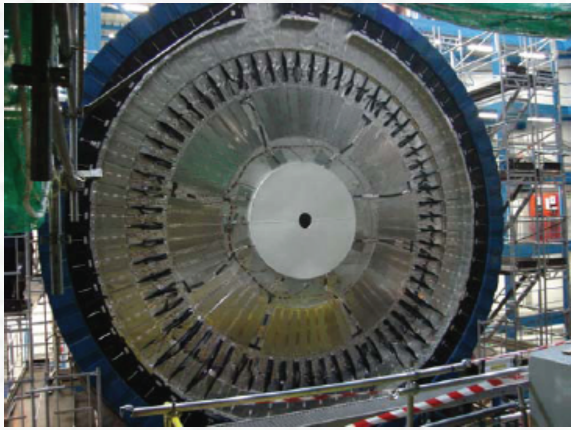

Some features of minimum bias events

- Features of minimum bias events cannot be calculated in perturbative QCD
- Experimental measurements / input needed
- Models / parametrizations were used to extrapolate from previous colliders (energies) to the LHC energy regime → large uncertainties
- Was one of the first physics measurements at the LHC
- Needed to model other interesting physics (superposition of events,…)

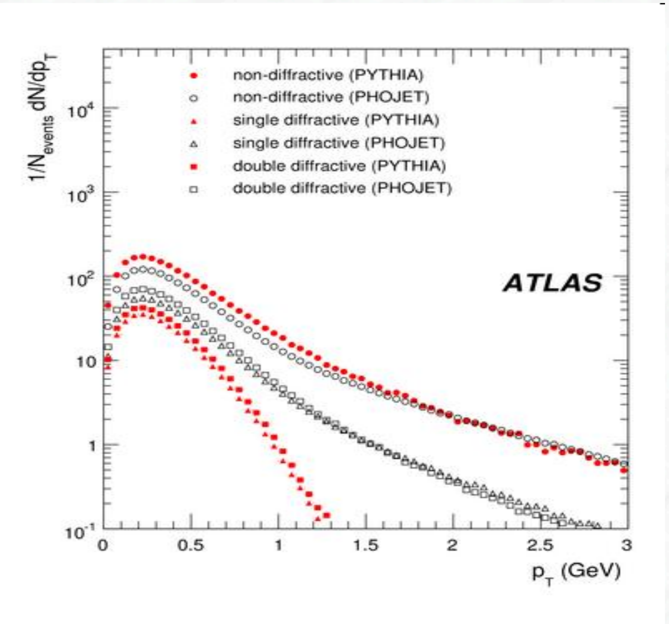

$\langle p_T \rangle$ (η =0): 550 – 640 MeV (15%)

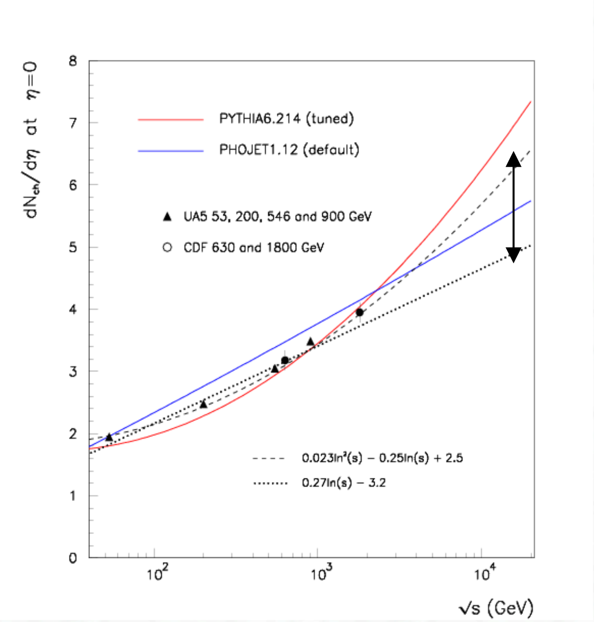

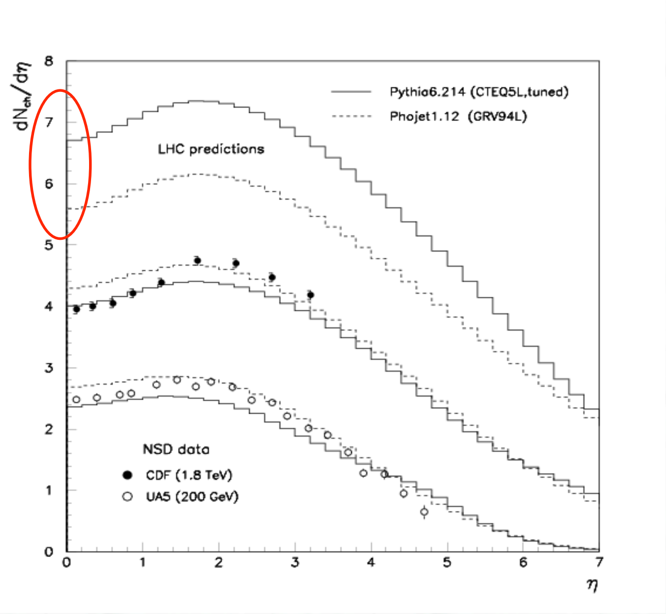

$dN_{ch}/d\eta$ (η=0): 5-7 (~ 33%)

First measurements from the LHC: datasets and selections

The Datasets:

$\sqrt{s}$=0.9 TeV (~7 μb-1)
- 360k events
- 4.5M tracks

$\sqrt{s}$=7 TeV (~190 μb-1)
- 10M events
- 210M tracks

The Event Selection:

- MBTS single-cell trigger in coincidence with the BPTX (beam pickup)
- 1 Vertex reconstructed
  - 2 tracks + Beam Spot
  - No pileup (secondary vertex with >3 tracks)
- Track quality cuts (hits)
- cut on the impact parameters at the primary vertex to exclude non primary tracks

Phase Space considered : (see arXiv:1012.5104v2 for more than these two)

Most inclusive
- ≥2 good tracks
- p_T > 100 MeV ; $|\eta| \leq 2.5$

Lower diffractive contribution
- ≥6 good tracks
- p_T > 500 MeV ; $|\eta| \leq 2.5$

Charged particle density versus η

N_{ch}: number of primary charged particles corrected to particle level, normalized to the number of selected events N_{ev}

0.9 TeV

and

7 TeV data

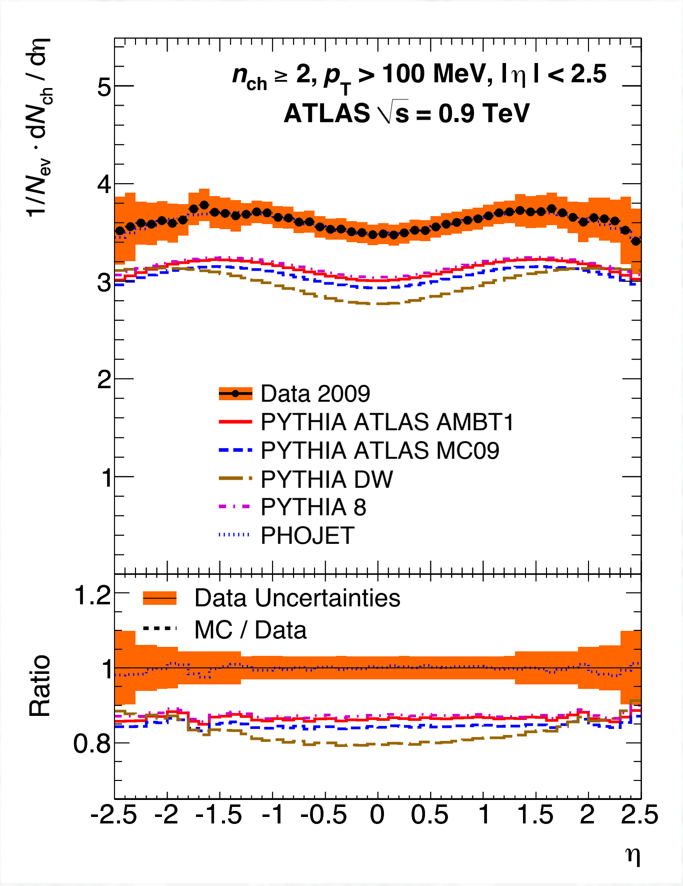

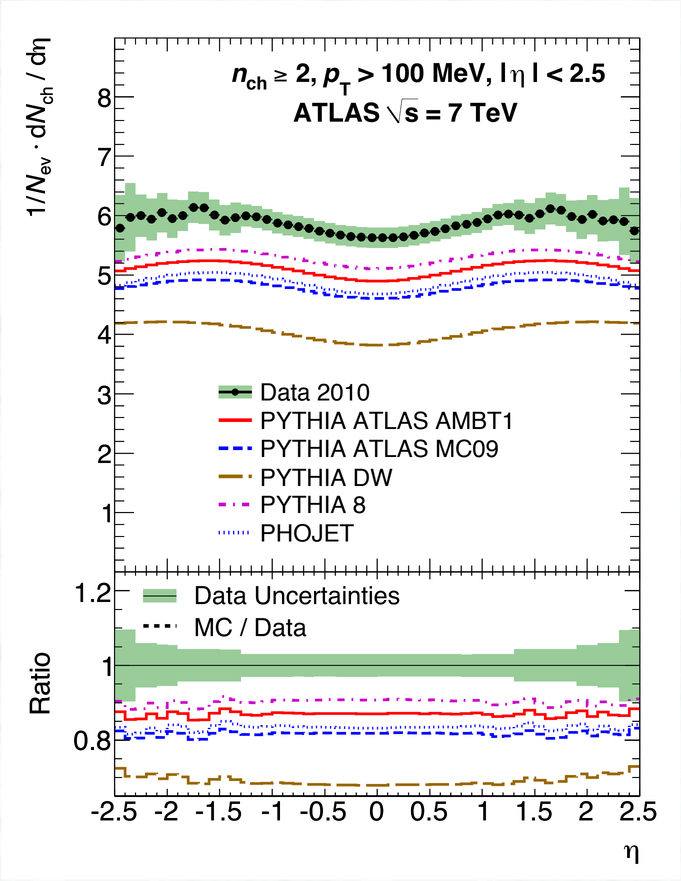

Various Monte Carlo models fail to describe the ATLAS data at both collider energies

Multiplicity distribution of charged particles

N_{ch}: number of primary charged particles corrected to particle level, normalized to the number of selected events N_{ev}

0.9 TeV

and

7 TeV data

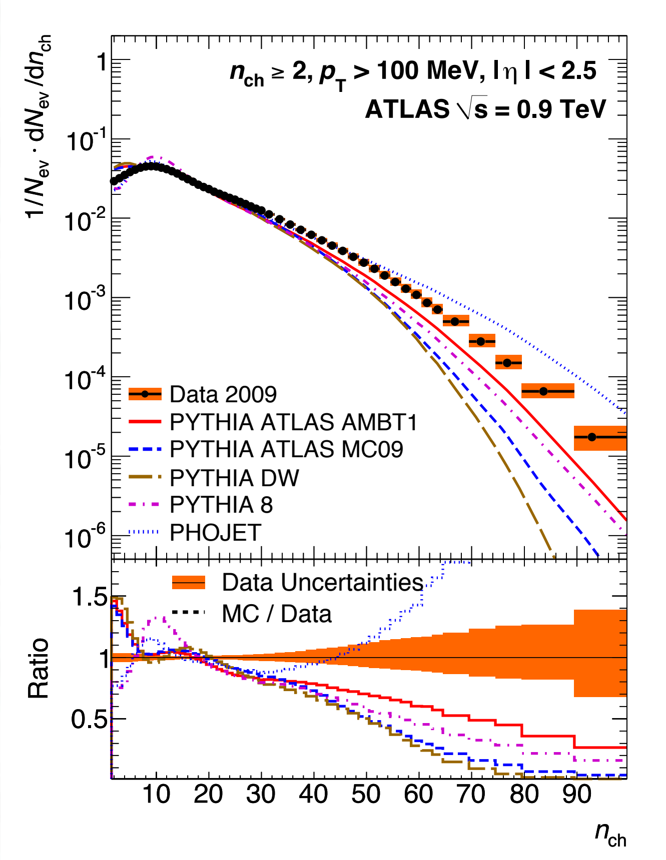

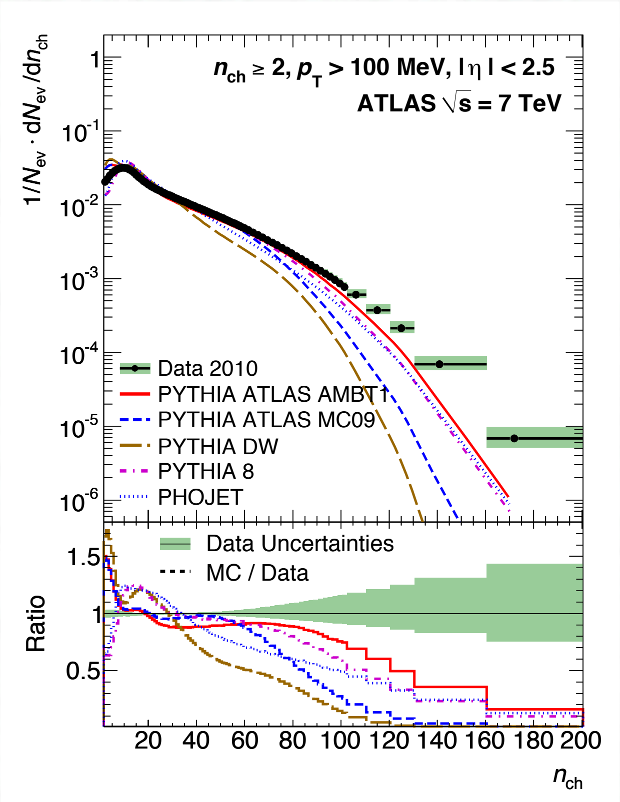

Various Monte Carlo models fail to describe high multiplicity events

Charged particle multiplicities as function of p_T

N_{ch}: number of primary charged particles corrected to particle level, normalized to the number of selected events N_{ev}

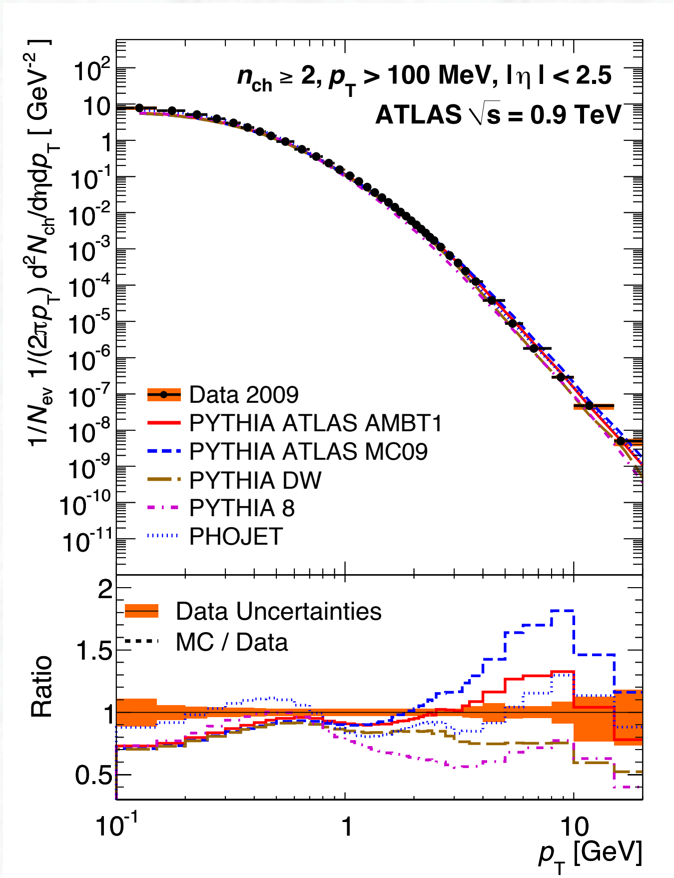

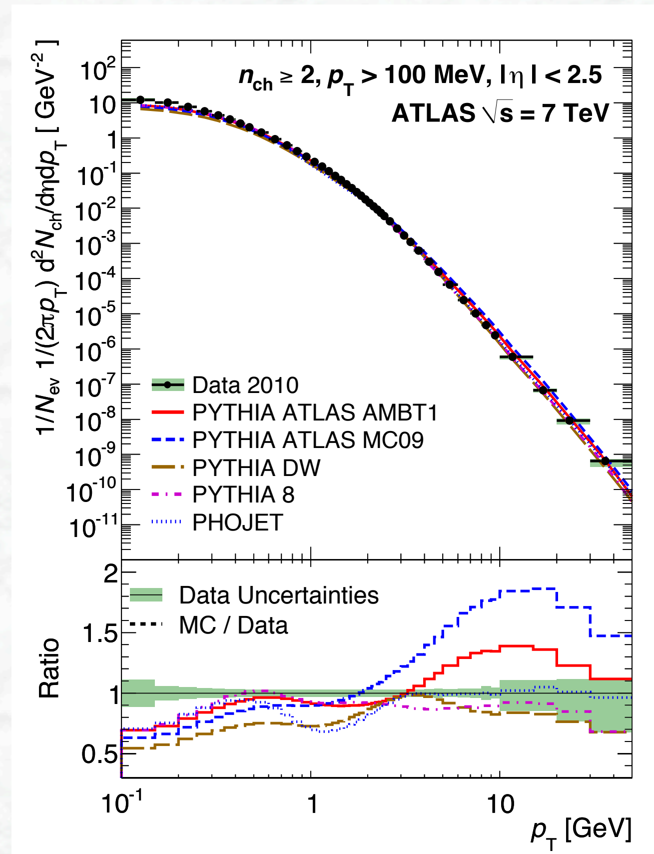

Monte Carlo models also fail to describe the p_T spectrum

The underlying event

Average charged particle density in transverse region

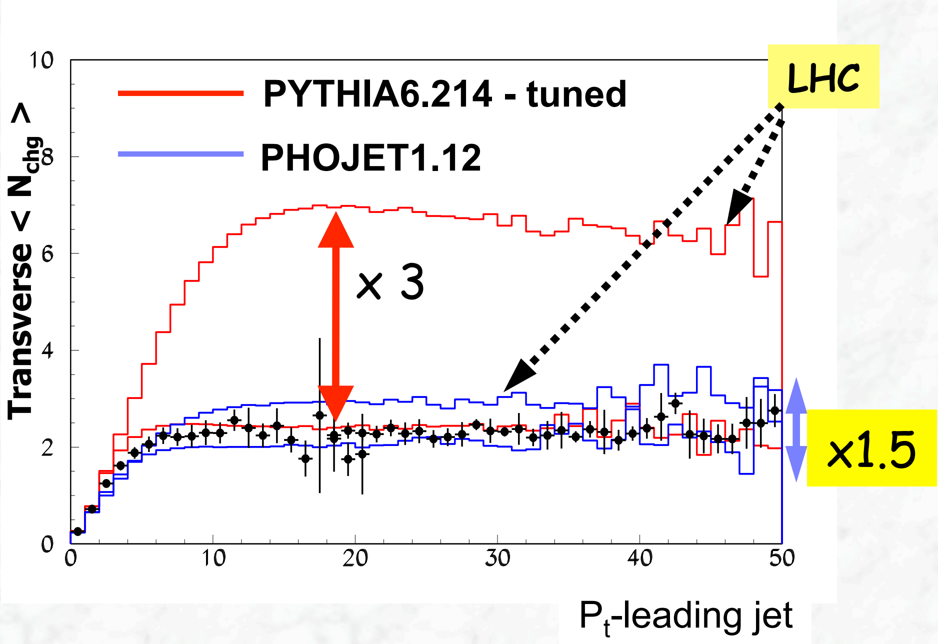

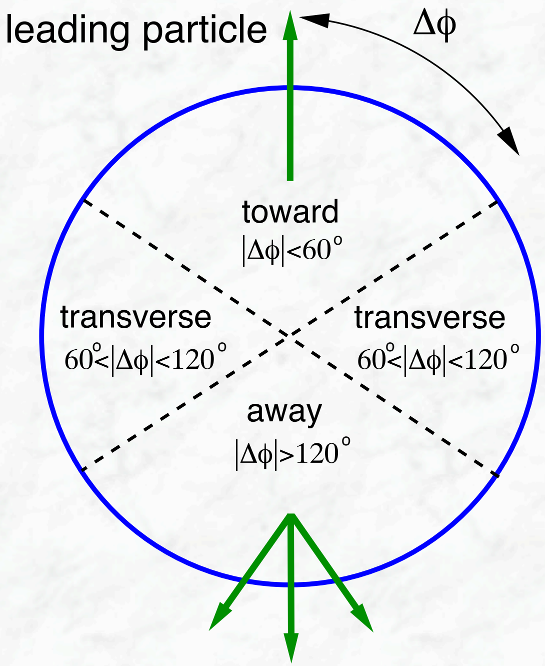

Extrapolation of the underlying event to LHC energies was unknown;

underlying event depends on:

- Multiple interactions
- Radiation
- PDFs
- String formation

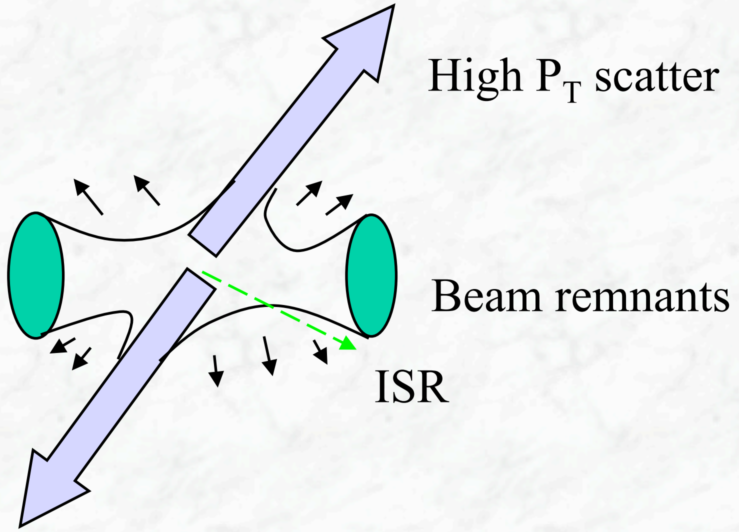

Measurements of underlying event properties with 7 TeV ATLAS data

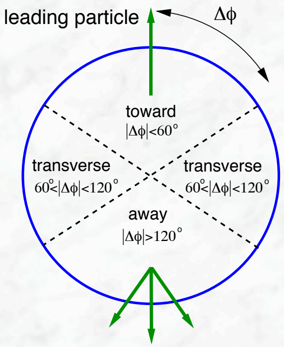

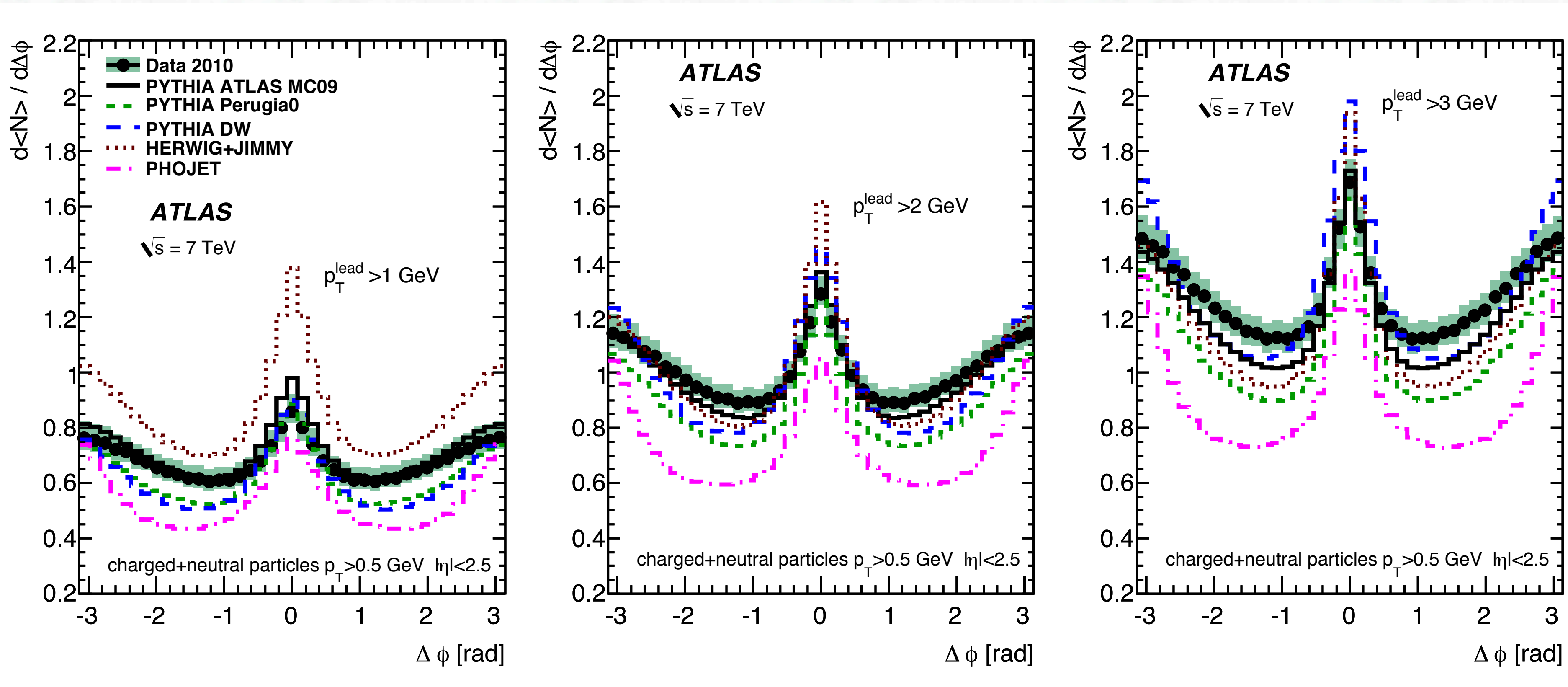

Measurements of underlying event properties with 7 TeV ATLAS data

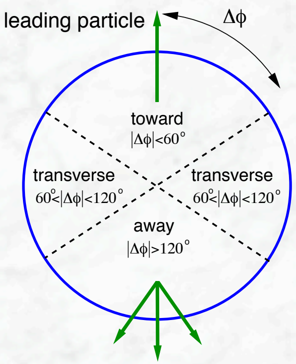

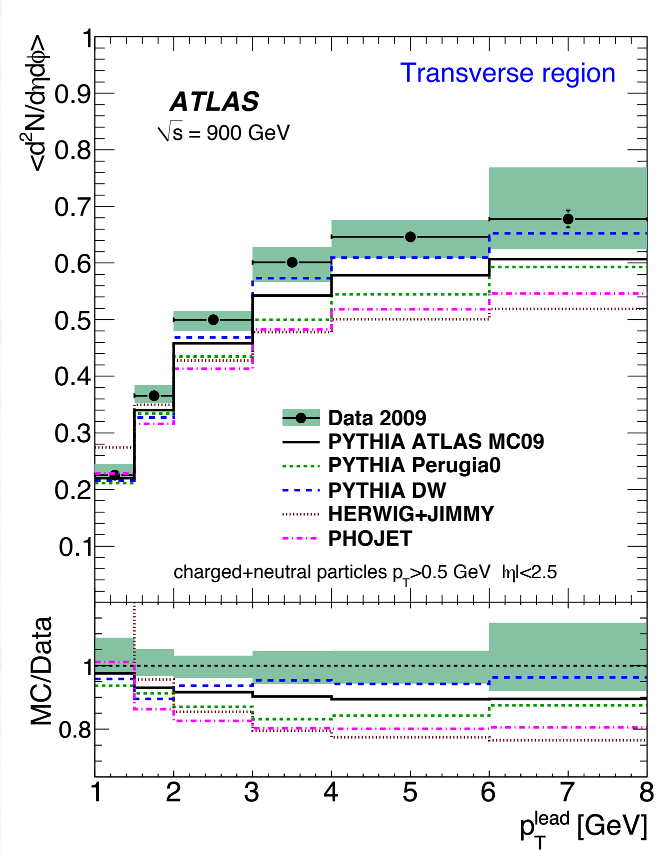

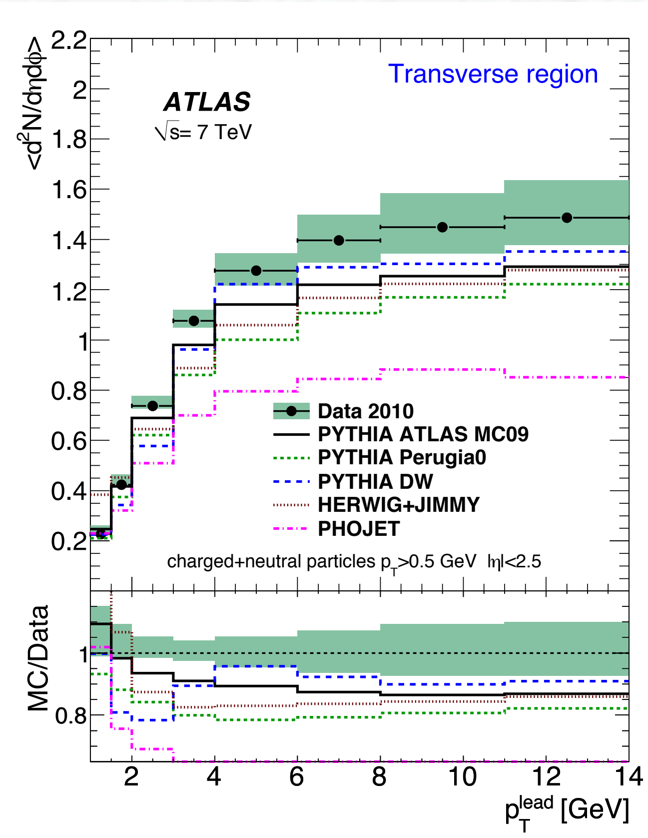

- number of particles (charged and neutrals) increase in the transverse region (plateau) by about a factor of two by going from 0.9 TeV to 7 TeV collisions
- models also fail to describe these features

➔ lot of tuning was needed and still needs to be done to parametrize the underlying event models including the necessary correlations